UNIVERSITY OF CALIFORNIA
Santa Barbara

A Physiological Unfolded Protein Response Impacts Progression Through the Cell Cycle

A Thesis submitted in partial satisfaction of the requirements for the degree of Master of Arts in Molecular, Cellular and Developmental Biology

By Soham Chowdhury

Committee in charge:

Professor Diego Acosta-Alvear, chair

Professor Kathleen Foltz

Professor Dzwokai Ma

March 2022

The Thesis of Soham Chowdhury is approved

Professor Kathleen Foltz

Professor Dzwokai Ma

Professor Diego Acosta-Alvear, chair

March 2022

A Physiological Unfolded Protein Response Impacts Progression Through the Cell Cycle

Dedication

I would like to dedicate this thesis to my mom, my dad, and my sister.

Without your love and support through the years, I would not be writing this today.

Acknowledgements

This thesis is a product of the guidance and mentorship of many people in my career so far. First and foremost, I'd like to thank Dr. Diego Acosta-Alvear. Your guidance and support through my first forays into laboratory research have shaped me as a scientist. You pushed me to think harder, strive farther, and to always expect the best out of myself. Your reminders to be playful with my science helped cultivate my scientific curiosity and always reminded me why I love science in the first place. I'd also like to thank Dr. Carolina Arias for your support as my unofficial co-PI. Thank you for always leading by example, and for cultivating a welcoming environment in our labs.

To Dr. Friederike Braig-Karzig, Fritzi: your mentorship ever since I joined the lab as an undergraduate has been foundational for my development as a researcher. You were infinitely patient early on as I learned basic research skills, and always pushed me to think critically and conduct my research systematically. You built me up when I struggled, and I so appreciate all of your kindness and support. I would not be where I am today without your help. I would also like to thank Dr. Kathy Foltz, for her guiding hand through my undergraduate and now graduate career at UCSB. You were one of the first people I went to for advice when I had no idea how to follow my dream of research, and your support and encouragement through the years has been invaluable as I worked towards my goals. To Dr. Zach Ma, thank you for all your help in crafting this thesis and for all your constructive feedback; I'm grateful for all our chats—both scientific and non-scientific— in the tissue culture room.

I would also like to thank Dr. Francesca Zappa for her scientific advice, her help in planning experiments and for always being willing to listen to and answer all my questions. I'm proud to have worked alongside such a skilled experimentalist. Additionally, I would like to acknowledge the help of Dr. Julien Bacal for his help with flow cytometry experiments and the Gardner and Richardson labs for allowing me to use their flow cytometer. Thanks also to Dr. Cassidy Arnold, for her technical support and insight and for allowing me to utilize the FACS equipment that was so central to this project.

A big thank you to everyone in the Acosta-Alvear and Arias labs: your feedback and support through the years as well as the collaborative environment we have created were central to my success here. And last, but not least: a big thank you to Sabrina Solley. Thank you for entrusting me to carry this project forward, thank you for all the support and advice, and for being a great friend. I'm proud to have worked with you on this project.

ABSTRACT

A Physiological Unfolded Protein Response Impacts Progression Through the Cell Cycle

By

Soham Chowdhury

The cell cycle is a series of coordinated molecular steps that allow a progenitor cell to produce two daughter cells. During symmetrical cell division, a mother cell's particular organelle makeup must also be inherited by the daughter cells. Multi-copy organelles such as mitochondria divide and are equally distributed between daughter cells. Single copy organelles such as the endoplasmic reticulum (ER) and the Golgi apparatus however must be first expanded, then fragmented, and finally partitioned to each daughter cell. Such organelle expansion requires the production of new membranes.

Being that the ER is the site of endomembrane biosynthesis, we reasoned that ER expansion should precede and be necessary for mammalian cell division. The Unfolded Protein Response (UPR) is an evolutionarily conserved collection of signaling pathways that maintain ER health. Protein folding perturbations in the ER lumen as well disturbances of the ER membrane lipid bilayer trigger ER stress and activate the UPR. The UPR mitigates ER stress by increasing the biosynthetic and protein degradative capacities of the ER, including its physical expansion through endomembrane biogenesis.

Here we show that as cells grow through interphase, their ER chaperone and foldase contents increase, as does the ER volume, indicating that ER expansion precedes cell division. Moreover, pharmacological inhibition of the UPR sensors IRE1 and ATF6 at steady-state

delayed cell cycle progression. Furthermore, we found that the threshold for UPR activation is lower in the S/G_2 stage of the cell cycle suggesting that ER expansion and increased ER protein-processing capacity is subsequent to genome duplication. Finally, our data indicate that IRE1 activity is dampened by the G_2/M cell cycle checkpoint kinase PKMYT1 suggesting negative feedback control. Taken together, these findings suggest a physiological role for the UPR in coordinating the mammalian cell cycle

Table of Contents

Project Background

The conception of this project was based on first principles about the requirements for symmetric cell division of mammalian cells. During symmetric division cells expand their single copy organelles (the ER and Golgi apparatus) so that they may be fragmented and partitioned evenly during mitosis. Defective inheritance of these organelles can result in a fitness cost to the progeny. Organelle expansion requires membrane biosynthesis. Since the ER is the site of membrane biogenesis (Uchiyama et. al. 1984), we focused on the ER health surveillance mechanism known as the unfolded protein response (UPR) and investigated the roles of the UPR in cell cycle progression.

In previous unpublished work (Solley, MA Thesis, UCSB, 2020), we generated several cell lines containing the Fast-FUCCI (Fluorescent Ubiquitination Cell Cycle Indicator) system that allows to fluorescently label cells in the G_1 and S/G_2 stages of the cell cycle (Koh et. al. 2017). Fast-FUCCI allows separation of these populations by flow cytometry and fluorescence activated cell sorting (FACS). Using this tool, we discovered an increase in chaperone and foldase content of the ER in S/G_2 cells, hinting at a role for the UPR— which upregulates chaperones and foldases—in coordinating the cell cycle. A pooled shRNA genetic screen for genes affecting the most conserved UPR sensor, the kinase/endoRNase IRE1, revealed a potential role for the G_2/M cell cycle regulator kinase PKMYT1 (Acosta-Alvear, unpublished). The work described in this thesis builds on these observations and aims at unraveling the interplay between the UPR and the control of the cell cycle, the differential sensitivity to ER stress between the stages of the cell cycle, and the mechanistic link between PKMYT1 and IRE1.

Introduction

1. Regulation of the mammalian cell cycle

The eukaryotic cell cycle is comprised of four distinct stages: G_1 (Gap 1), S (Synthesis), G_2 (Gap 2), and M (Mitosis). Most of the cell cycle is comprised of the G_1, S and G_2 phases of the cell cycle (collectively termed interphase) after which mitosis unfolds quickly. Each of the stages of the cell cycle is characterized by a synchronous set of molecular events that allow the cell to progress from one stage to the next once all self-checks are successfully met (Alberts et. al. 2015). These "checkpoints" integrate information about internal and external cues to make the decision of whether or not to divide. Cell cycle checkpoints oversee genome integrity, organelle content, cell size, and nutrient availability.

Cell division may be symmetric or asymmetric depending on how cellular contents are distributed. Symmetric cell division gives rise to identical daughter cells and is important for proliferation and maintenance of tissues, while asymmetric cell division is required to establish different cell identities from a common progenitor cell (Shahriyari and Komarova et. al., 2013).

To integrate this breadth of information, a variety of cellular signaling networks are interleaved with the cell cycle. For example, stress signaling pathways that respond to oxidative stress, DNA damage, nutrient deficiencies, and the cellular environment all feed into the cell cycle. In healthy cells, this tight multilayered regulatory system allows damaged cells to pause and attempt to restore homeostasis before undergoing cell division (Ishikawa et. al., 2007; Macip et. al., 2006; Rohde et. al., 2001). In this way, cells that are irreparably damaged are purged. When these regulatory systems are compromised, cells that should have been cleared continue dividing, which can lead to cancer (Collins et. al., 1997).

The G_1 phase of the cell cycle is governed by the actions of Cyclin D1 in complex with the cyclin-dependent kinases CDK4 or CDK6 (Satyanarayana and Kaldis et. al., 2009). Cells evaluate nutrient availability and induce the expression of Cyclin D1 if resources are adequate (Gerard and Goldbeter et. al., 2014). If conditions are not optimal, cells can enter a fifth stage, known as G_0. This fifth stage, G_0, comprises a cellular state outside of the replicative cell cycle. Cells can enter G_0 from the G_1/G_0 restriction point and either (1) remain in G_0 indefinitely as part of their normal developmental program (as occurs in post-mitotic terminally differentiated cells, such as neurons or muscle cells), (2) remain in G_0 indefinitely as part of the process of senescence, or (3) remain in G_0 temporarily as quiescent cells that can reenter the cell cycle when favorable conditions for division are met (Pardee et. al., 1974).

If conditions are permissive to division, Cyclin D1/CDK complex will phosphorylate the Retinoblastoma tumor suppressor protein (Rb), leading to a de-repression of the E2F transcription factors that in turn drive the expression of Cyclins E and A that are required for cells to enter the S phase of the cell cycle (Kato et al., 1993; Satyanarayana and Kaldis et. al., 2009; Weinberg et. al., 1995). Cyclin E and A complex with CDK2 to activate the DNA replication machinery (Coverley et. al., 2002). In S phase, DNA damage and repair pathways ensure that genome duplication is carried out with fidelity. Failure to faithfully duplicate the genome results in cell cycle arrest in S phase and the initiation of programmed cell death.

Once the genome has been duplicated successfully, cells enter G_2. In G_2 the integrity of the genome continues to be monitored, and the cell grows in preparation for division. Cyclin A and Cyclin E continue to orchestrate events through this stage by complexing with CDK1 and inducing the expression of Cyclin B1 which will eventually promote entry into mitosis (Jeffrey et al., 1995). Events such as the fragmentation of single copy organelles, and

cytoskeletal rearrangements are essential for proper cell division occur in G_2 (Oullet et. al. 2012).

Mitosis is comprised of five stages: prophase, prometaphase, metaphase, anaphase, and telophase which together orchestrate a dramatic reorganization of cellular components to partition them into two daughter cells. In prophase, chromatin condenses, and the nuclear envelope breaks down. In some ancient unicellular eukaryotes, such as *S. cerevisiae*, the nuclear envelope does not break down and instead the intact nucleus is divided in two in a process termed "closed mitosis" (Boettcher and Barral et al., 2013). In prometaphase, a transitionary period between the breakdown of the nuclear envelope and the formation of the metaphase plate, microtubules attach to the kinetochores in the condensed sister chromatids to form the mitotic spindle. The master regulator of metaphase is the complex comprised of CDK1 and Cyclin B1 known as the Maturation Promoting Factor (MPF), which phosphorylates key structural proteins to enable cellular reorganization (Maller et al., 1989). CDK1 directly phosphorylates histones and nuclear lamins, enabling both chromatin condensation and nuclear envelope disassembly (Boulikas et al., 1995). The fragmentation of the Golgi apparatus and ER also occurs in this stage and there is some evidence that the MPF also promotes this process (Lowe et. al., 2000). However, the mechanism by which these organelles are fragmented remains elusive. Once the mitotic spindle forms, it attaches to each chromatid from a centrosome at each pole in the cell so that they may be segregated into the two daughter cells. After the spindle is assembled and the chromatids align at the metaphase plate, the cell is in metaphase and ready to segregate its genetic material.

The spindle assembly checkpoint in the metaphase to anaphase transition is critical since improper genome segregation leads to aneuploidy, a hallmark of cancer. The Anaphase

Promoting Complex (APC) is a ubiquitin ligase complex that is induced by the MPF in early metaphase but is kept inactive until anaphase. The APC degrades the MPF and ubiquitylates a protein called securin that acts as an inhibitor for the protease separase. De-repression of separase licenses the separation of the sister chromatids by the coordinated action of cytoskeletal and motor proteins. The APC also degrades Cyclin B which leads to the inactivation of the MPF and mitotic exit in telophase (Castro et. al., 2005). Telophase comprises of the reversal of mitotic events that were induced by the MPF and the reorganization of cellular compartments as the two daughter cells prepare to separate. The nuclear envelope reforms, chromatin decondenses, and the cytoskeleton returns to an interphase state. Cytokinesis marks the end of mitosis as an actin-myosin contractile ring at the cell's midbody drives abscission and separation of the two daughter cells (Cheffins et. al., 2016).

The regulation of the cell cycle depends on the tight temporal regulation of cyclin expression so that the correct cyclin/CDK complexes can be formed at each stage. CDK inhibitors of two families (INK4 derived, and Cip/Kip derived) bind Cyclin/CDK complexes to inactivate the CDK and hold the complex in a non-functional state while the cell attempts to correct any defects (Hunter and Pines et al., 1994). Unsurprisingly, both families of CDK inhibitors are induced by cellular stress such as DNA damage and viral infection which allows the cell to pause in a stage of the cell cycle in an attempt to restore homeostasis before proceeding with cell division (Besson et al., 2008; Gartel and Tyner et al., 1999; Sherr and Roberts et al., 1999). The INK4 derived CDK inhibitors are specific to CyclinD/CDK4 or CyclinD/CDK6 complexes, while the Cip/Kip CDK inhibitors are more promiscuous and have several Cyclin/CDK complex substrates (Canepa et al., 2007; Hunter and Pines et al., 1994).

Another layer of regulation is derived from the phosphorylation status of CDKs within these complexes. A particularly well characterized example is the regulation of the CyclinB1/CDK1 complex by the kinases CAK, Wee1, and PKMYT1. CAK phosphorylates threonine 161 in CDK1 upon entry into G_2, which is a modification required for the MPF complex to initiate mitosis (Ducommun et al., 1991; Fesquet et al., 1993). CDK1 can also be phosphorylated to negatively regulate mitotic entry, an effect mediated by the activity of the Wee1 family of kinases consisting of Wee1, Wee1B, and PKMYT1 (Schmidt et al., 2017). These kinases phosphorylate CDK1 in response to DNA damage causing a cell cycle arrest at the G_2/M transition (Liu et al., 1997; Russell and Nurse et al., 1987). Wee1 and PKMYT1 can both phosphorylate Tyr15 on CDK1, and PKMYT1 can additionally phosphorylate Thr14. If the stress is resolved by DNA repair pathways, CDC25 phosphatases can restore CyclinB/CDK1 to its active state to allow progression through mitosis (Hoffmann et al., 2000). Therefore, the Wee1 family of kinases along with CDC25 exert regulatory control over the G_2/M transition.

2. Cell Size Sensing and Organelle Inheritance During the Cell Cycle

As cells proceed through interphase, they grow in preparation for cell division. Furthermore, distinct cell types have characteristic sizes suggesting tight regulatory control to ensure that progeny cells are sized appropriately. This observation suggests a mechanism for cells to sense their size and either add or subtract mass to ensure properly sized daughter cells (Rishal, Fainzilber et. al. 2019; Fantes and Nurse et al., 1977; Killander and Zetterberget al., 1965). While a mechanism has yet to be defined for this process, three models of cell size sensing have been proposed. In the first model, referred to as the "adder model", cells of different sizes

add a constant amount of material prior to each division. In this model, cell sizes are not individually adjusted prior to each cell division but rather that the cell population reaches a steady state cell size over successive divisions (Conlon and Raff et al., 2003). The second model, termed the "sizer model" postulates that cells titrate their size by sensing the intracellular concentrations of key cell cycle regulators to establish thresholds for when to start or stop growing (Facchetti et. al. 2017). Under the third model, called the "timer model", cells do not explicitly sense their size, but grow for a certain constant amount of time (Rishal, Fainzilber et. al. 2019).

Neither the "adder" nor "timer" models require the existence of an active size sensing mechanism, but the "sizer" model does. It is plausible that the three models are not mutually exclusive but could act in concert to regulate cell size. Post-mitotic cells such as neurons grow to a characteristic size, suggesting that sizer-like mechanisms or extrinsic signals regulate cell size. There is evidence for all three proposed models, however there is no consensus yet whether there is a universal mechanism for cell size sensing in mammalian cells. Furthermore, mammalian cell cultures studies have traditionally been restricted to a two-dimensional context rather than the three-dimensional one they exist in naturally. This complicates studies of the cell cycle since an essential aspect of the physiological system is missing in the in vitro model: there could very well be spatial cues enabled by three dimensional contacts that enable size-sensing and inform decisions about cell cycle progression. Three-dimensional mammalian cell culture systems may provide more insight into these mechanisms in future studies.

Besides cell growth, symmetrical cell division requires that organelles also be divided (as in the case of multi-copy organelles such as mitochondria) or expanded and fragmented (in the case of single-copy organelles such as the ER and Golgi apparatus) to ensure the proper

inheritance of organellar content (Warren and Wickner et al., 1996). There is strong evidence for the multiplication of organelles such as mitochondria and peroxisomes by fission to stochastically partition roughly equivalent amounts of organelles per each daughter cell (Moore et. al. 2021; Warren and Wickner et al., 1996; Birky et al., 1983). In single copy organelles such as the Golgi apparatus, fragmented membranes have been shown to be associated with the mitotic spindle, suggesting an ordered rather than stochastic model of organelle partitioning (Shima et al., 1998). Additionally, the reassembly of the Golgi apparatus has been linked mechanistically to the activity of the aforementioned G_2/M regulator kinase PKMYT1 (Nakajima et al., 2008). This observation suggests that organelle inheritance may be integrated with the well-characterized cell cycle checkpoints. Whether or not these events make up distinct checkpoints in the cell cycle or whether they are part of the checkpoints already characterized remains to be determined (Colanzi et al., 2007).

The ER also undergoes dramatic reorganization during mitosis and given that the ER is the site of lipid biogenesis it follows that the ER is a major regulatory hub for the proper inheritance of any organelles that require *de novo* membrane synthesis. Newer studies have also implicated the ER in the coordination of mitochondrial and endosomal division through ER-organelle contact sites and given the ER's close connection with the Golgi apparatus, it is surprising that an ER integrity checkpoint has not been yet described for the cell cycle (Adachi et. al. 2020).

3. The Endoplasmic Reticulum and the Unfolded Protein Response

The endoplasmic reticulum (ER) is the largest contiguous organelle in the cell and the site for lipid biogenesis, calcium buffering, and secreted and transmembrane protein biosynthesis. The

ER can be divided into two topologically distinct domains, the nuclear envelope, and the peripheral ER (Hetzer et al., 2005). The nuclear envelope encloses the genetic material in the cell and is biochemically and biophysically distinct from the peripheral ER. The nuclear envelope consists of a double lipid bilayer: the outer nuclear membrane (ONM) and the inner nuclear membrane (INM). The INM is distinct from the ONM in protein composition because of selective retention mechanisms inside the nucleus. The ONM however, which is also contiguous with the peripheral ER, has a protein composition that is similar to that of the peripheral ER (Ellenberg et al., 1997; Gerace and Burke et al., 1988; Newport and Forbes et al., 1987; Soullam and Worman et al., 1995). The peripheral ER can be further subdivided into two functional types: smooth and rough ER, which are characterized by the absence or presence, respectively, of ribosomes and the protein translocation machinery. The relative levels of rough versus smooth ER in a particular cell type depends on the cell's functional niche (Shibata et al., 2010; Shibata et al., 2006). For example, plasma cells that are highly specialized for antibody secretion have extensive rough ER that occupies most of the cell's volume (Gass et al., 2004; Kirk et al., 2010). In contrast, cells that have a greater need for lipid production such as hepatocytes have mostly smooth ER which is responsible for lipid biogenesis and transport (Uchiyama et. al. 1984; Loud et. al. 1968).

The morphology of the ER varies within the cell, with the peripheral ER closest to the nucleus being composed mainly of flat sheetlike cisternae, and the distal ER composed mainly of a mesh of highly interconnected and dynamically remodeled tubules. ER shaping proteins such as those in the Reep and CLIMP families can dynamically remodel ER into more tubular or more sheet-like morphologies depending on the cell's biosynthetic requirements (Gurel et. al. 2014). There is also evidence that regions of the ER can form nanodomains with distinct

biochemical makeups. By partitioning ER machinery with specific functions (such as export of cargo to the Golgi apparatus) the ER can form functional niches within the organelle (Gao et. al. 2019).

As the ER network is distributed through the entirety of a cell's volume, it also establishes membrane contact sites with other organelles in the cell, the plasma membrane, and some membrane-less organelles such as P-bodies and stress granules (Lee et. al 2020, Abrisch et. al. 2020, Lewis et. al. 2016). Therefore, the ER can be thought of as a hub of inter-organelle communication. These contact sites likely coordinate multiple molecular events. For example, lipid biogenesis and metabolism are coordinated by the ER as well as the mitochondria, and there is evidence that ER-mitochondrial contact sites serve a role in the metabolism of lipid precursors as well as lipid transfers between organelles (Kornmann et al., 2009; Jelsema, Morre, et al 1978). ER-lysosome contact sites have been shown to be signaling hubs that enable cholesterol sensing by mTORC1 (Lim et. al. 2019). There is also evidence suggesting that ER-peroxisome contact sites are important for peroxisome biogenesis and function (Costello et. al. 2017). An intriguing possibility is that the ER mediates three-way or multi-way contacts between different organelles such as peroxisomes and mitochondria, both of which have roles in cellular redox metabolism (Chen et. al. 2020; Friedman et al., 2011). Furthermore, ER-organelle contact sites have also been shown to play an important role in the fission of mitochondria and endosomes (Adachi et. al. 2020; Rowland et al., 2014). ER-plasma membrane contact sites have also been shown to be important in phosphatidylinositol signaling, ion exchange, and cell motility (Scorrano et. al. 2019; Manford et al., 2012). The connection between the ER and the Golgi apparatus is perhaps the best characterized of all organelle

interactions: the entire secretory pathway relies on the proper communication between these two organelles.

Protein export in the secretory pathway occurs in an anterograde direction with layers of quality control to ensure only properly folded cargoes leave the ER (Braakman et. al., 2013). Protein cargoes mature by sequential modifications: first in the ER, then the ER-Golgi Intermediate Compartment (ERGIC), and finally in the Golgi apparatus (Appenzeller-Herzog et al., 2006). The secretory pathway is shut off during mitosis in order to prevent improper targeting of cargo (Yeong et. al., 2013). Taken together, these observations suggest a central role for the ER in the maintenance and inheritance of cellular organelle content. The structure of the mitotic ER has been a source of debate and the evidence is still unclear as to how ER structure is reorganized during division. Some studies suggest a complete disassembly of the nuclear envelope and partial vesiculation of the rest of the ER (Jokitalo et. al., 2001), others suggest that the mitotic ER is comprised mainly of extended sheets (Bergman et. al., 2015). In either case, the ER's morphology undergoes dramatic changes during mitosis, and therefore it is attractive to speculate that ER inheritance is subject to multiple layers of regulatory control ranging from fragmentation, establishment of specific topological niches, and organelle contact sites. More work is required to understand the structural changes, partitioning, and eventual re-consolidation of the ER after mitosis.

The ER is also a major hub of protein synthesis. Roughly 30% of the proteome is comprised of secreted and transmembrane proteins that are synthesized in the ER (Uhlén et. al., 2015). Thus, the ER is equipped with a vast array of translation and quality control machineries that ensure the maintenance of the cell's secreted and transmembrane proteomes. Most proteins are targeted to the ER co-translationally upon recognition of an N-terminal

hydrophobic peptide sequence by the Signal Recognition Particle (SRP) which pauses translation of the nascent polypeptide and translocates the ribosome-mRNA-peptide complex to the ER via interactions with the SRP receptor (Shen et. al., 2010). Proper interactions of the cargo within the SRP and SRP receptor complex slow down the GTP hydrolysis and recycling of the complex long enough for the translocon to be engaged. Once engaged, the ribosome and cargo are docked to the Sec61 translocon and the nascent peptide is inserted into the translocon tunnel. Translation resumes, now coupled with translocation into the ER lumen, and the SRP-SRP receptor complex is recycled (Walter and Blobel et al., 1981). Once in the ER lumen, ER chaperones and foldases assist the folding of the newly minted peptides (Braakman and Hebert et al., 2013). Proteins that do not fold correctly are targeted for degradation via a process known as ER-associated degradation (ERAD) (Qi et. al., 2017).

The ER harbors lipid synthesis enzymes that are required to produce lipid membrane precursors. The ER also enables the formation of lipid droplets, which are lipid storage vesicles enclosed by a phospholipid monolayer (Olzmann and Carvalho et al., 2019). In addition, the ER is the major site of calcium storage in the cell, where it both provides a favorable redox environment for proper protein folding and a calcium buffering system to initiate signaling events (Carreras-Sureda et. al., 2018). Calcium ions are a key second messenger in cellular events such as neurotransmitter release, muscle contraction, cell motility and growth, and allosteric modulation of enzyme activities. If cytosolic calcium concentrations are too high, the ER reuptakes calcium through channels known as SERCA pumps. ER calcium release can

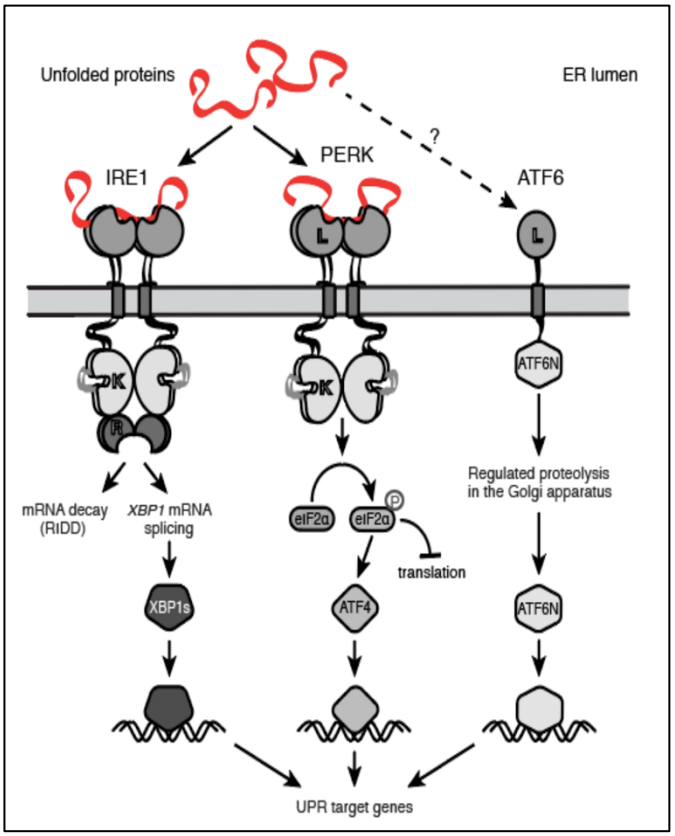

Fig 1. The Unfolded Protein Response pathway. The three sensors IRE1, PERK, and ATF6, as well as their outputs after activation are depicted. (Karagöz et. al. 2019)

also fine tune mitochondrial function and titrate the threshold for apoptosis in response to stress (Pinton et. al., 2010).

The Unfolded Protein Response (UPR) is an evolutionarily conserved homeostatic mechanism that monitors the protein folding capacity of the ER and adjusts ER functions according to the cell's needs (Karagöz et. al., 2019, Walter and Ron et al., 2011). The mammalian UPR consists of three signaling branches governed by three transmembrane ER stress sensor proteins: PERK, IRE1, and ATF6 (Figure 1, Karagöz et. al., 2019). PERK is a transmembrane kinase that is also a part of the Integrated Stress Response (ISR); a central homeostatic mechanism that detects multiple stresses (Costa-Mattioli et al., 2020). Upon detection of unfolded proteins in the ER, PERK oligomerizes and is auto-phosphorylated in the plane of the ER membrane (Harding et. al. 1999). Active PERK phosphorylates the eukaryotic initiation factor 2α (eIF2α), which leads to global protein synthesis shutdown and a reduction in ER protein folding load (Marciniak et. al., 2006; Prostko et. al., 1993). Phosphorylation of eIF2α paradoxically upregulates the translation of select mRNAs harboring upstream open reading frames in their 5' UTRs, the best characterized of which is the bZIP transcription factor ATF4, which induces genes that increase

the cell's biosynthetic capacity (Vattem and Wek 2004). ATF4 also induces the pro-apoptotic transcription factor CHOP, which controls cell fate when the stress cannot be resolved (Rozpedek et. al., 2015). In this way, ATF4 integrates information about stress to control cell survival or death.

IRE1 is the most conserved of the three UPR sensors and is a transmembrane kinase/endoRNase (Cox et. al., 1993). IRE1 possesses an ER lumenal sensor domain that recognizes unfolded proteins by direct binding and is fine-tuned by a reversible association with the ER chaperone BiP (Credle et. al., 2005, Karagoz et. al., 2017). When the protein folding environment in the ER is favorable and unfolded clients for BiP are in low abundance, BiP is unengaged and can bind to and sequester inactive IRE1 monomers so that the UPR is not spuriously activated (Pincus et. al., 2010). When IRE1 detects unfolded proteins, it oligomerizes in the plane of the ER membrane, trans-autophosphorylates and allosterically activates its cytosolic RNase domain. Active IRE1 excises an unconventional 26 nucleotide intron from the *XBP1* mRNA at a canonical CNGNNGN motif (Peschek and Acosta-Alvear et al., 2015; Korennykh et. al., 2011; Gonzalez et. al., 1999). The exons are ligated by the tRNA ligase RTCB (Kosmaczewski et. al., 2014; Lu et. al., 2014) This splicing reaction causes a frameshift in the *XBP1* mRNA that allows the translation of a potent bZIP transcription factor referred to as XBP1s (s for "spliced"). The structure of the *XBP1* mRNA is important for the splicing reaction as a conformational RNA zipper structure is required for efficient cleavage and intron excision (Peschek, Acosta-Alvear et. al., 2015). XBP1s controls a vast gene expression program that increases the ER lipid biosynthetic and protein-degradative capacities (Acosta-Alvear et al., 2007). Overexpression of XBP1s physically enlarges the ER by increasing lipid biosynthesis (Sriburi et al., 2004). XBP1s also controls genes not immediately

related to ER physiology such as genes involved in DNA repair, suggesting that it coordinates multiple cellular pathways to restore homeostasis (Acosta-Alvear et al., 2007).

IRE1 also cleaves ER-bound mRNAs in a process known as Regulated IRE1 Dependent Decay (RIDD) (Hollien and Weissman et al., 2006). RIDD is thought alleviate an overburdened ER by reducing incoming protein loads. However, a recent finding challenges this notion. The *Blos1* mRNA, encoding a lysosome trafficking factor is a canonical RIDD substrate whose degradation allows the repositioning of lysosomes to clear protein aggregates (Bae et. al., 2019). Emerging evidence supports the notion that RIDD is a more general mechanism for RNA homeostasis rather than a simple ER load buffer (Dufey et. al., 2020). IRE1 is also a key sensor of lipid perturbations in the ER. Changes in ER membrane lipid composition and in particular the degrees of saturation in the constituent membrane lipids can cause variations in membrane thickness, which results in membrane deformation that IRE1 senses through its transmembrane amphipathic helix. These membrane deformations push IRE1 monomers together in self-association resulting in activation (Halbleib et. al., 2017). IRE1 activation via lipid bilayer stress induces a different transcriptional program than is induced when IRE1 is activated by unfolded protein stress (Ho et al., 2020). Although these perturbations are recognized by different sensor domains of IRE1 (an amphipathic transmembrane helix, and the ER lumenal domain respectively), self-association and phosphorylation of IRE1 monomers is the mechanism that activates IRE1 in both cases. This suggests that IRE1 is able to integrate information about the triggering stimulus into its output.

ATF6 is a transmembrane protein that traffics to the Golgi apparatus upon ER stress where it undergoes proteolytic processing by the S1P and S2P proteases. This regulated proteolysis liberates a soluble N-terminal bZIP transcription factor (ATF6-N) that induces ER

biosynthetic and ERAD genes (Yoshida et al., 1998; Haze et al., 1999; Ye et al., 2000). Although the precise mechanism of ATF6 activation is still unknown, there is evidence that suggests that ATF6 might be coupled to redox sensing (Nadanaka et. al., 2007). Moreover, XBP1s and ATF6-N can homodimerize or heterodimerize to combinatorially induce UPR target genes, suggesting transcriptional fine tuning in response to the specific cellular needs (Yamamoto et. al., 2004).

If ER stress cannot be resolved, the UPR switches to drive apoptosis by the induction of the transcription factor CHOP downstream of the PERK- ATF4 branch (Lu et. al., 2014). CHOP in turn induces death receptor 5 (DR5), which signals unconventionally from the Golgi apparatus to drive a cell-autonomous apoptotic program (Hu et. al., 2019). The DR5 mRNA is also a RIDD substrate, so the terminal UPR involves a molecular clock in which DR5 expression is counterbalanced by IRE1's protective actions through RIDD (Lu et. al., 2014).

4. UPR dysregulation in disease

A dysfunctional, overridden, or maladaptive UPR can lead to a variety of disorders. The dysregulation of the UPR has been implicated in protein folding disorders such as Alzheimer's disease, prion-related diseases, Parkinson's disease, and Polycystic Kidney Disease among others (Duran-Aniotz et. al., 2014; Hashida et. al., 2012; Hetz and Mollereau 2014; Matus et. al., 2013; Roussel et. al., 2013; Vidal and Hetz 2012; Wang et. al., 2012). Many stress inputs not directly related to protein folding homeostasis nevertheless impact ER physiology. Such conditions include hyper-homocysteinemia, hyperglycemia, and hyperlipidemia (Werstuck et. al., 2001). These diverse conditions, together with *bona-fide* protein folding perturbations (i.e, ER overload, or mutant proteins that cannot be properly folded) converge on a disruption of

the ER homeostasis and activation of the UPR. Therefore, UPR signaling can be tied closely to the etiology of a wide variety of diseases.

The importance of the UPR is most appreciated in specialized secretory cells. For example, pancreatic β cells are heavily reliant on proper ER function, and specifically IRE1's RIDD activity in order to secrete insulin (Scheuner et. al., 2001). In cancers of specialized secretory cells such as multiple myelomas, overexpression of the IRE1/XBP1s axis and suppression of apoptotic signaling are coupled, presumably endowing the cancer cells with the ability to deal with their secretory burden (Harnoss et. al., 2019). In osteosarcomas, aberrant activation of the UPR primarily through the ATF6 branch promotes tumor survival in the face of chemotherapeutic challenge and increases their metastatic potential (Yarapureddy et. al., 2019). From these observations it follows that a maladaptive UPR gives a growth and survival advantage to cancer cells, and hence, cancer cells can be thought of as a good model system to study the interconnectivity of the UPR with the cell cycle machinery.

5. The Fast FUCCI system as a tool to visualize stages of the cell cycle

Studying the cell cycle status of an asynchronous population requires the use of DNA intercalating agents such as propidium iodide or 4′,6-diamidino-2-phenylindole (DAPI). Changes in the cell cycle distribution can be assessed based on the proportion of cells with n (G_1), 2n (G_2) or intermediate levels of DNA content (S). However, this method does not allow to physically separate cells in each cell cycle stage for subsequent biochemical analysis. Methods that are able to separate cells into distinct stages in the cell cycle exploit the natural cell cycle checkpoint machinery to synchronize populations of cells using cell cycle disruptors such as nutrient deprivation, which forces cells into quiescence and causes an arrest at the

G_1/G_0 restriction point, and culturing cells in media supplemented with thymidine, which disrupts deoxynucleotide biosynthesis, preventing DNA replication and arresting cells at the G_1/S checkpoint (Reichard et. al., 1962). Pharmacological cell cycle disruptors are also routinely used. For example, microtubule depolymerizing agents, such as nocodazole, destabilize the mitotic spindle and cause cells to fail the spindle assembly checkpoint and arrest cells at the G_2/M transition. Aphidicolin, a fungus derived diterpenoid, selectively blocks DNA Polymerase α, preventing DNA synthesis and arresting cells at the G_1/S checkpoint (Borel et. al., 2002). Mechanical means to select for cells at different stages of the cell cycle can also be used. For example, in a technique known as "mitotic shake-off", mitotic cells can be selected from a population of adherent cells by mechanically dislodging loosely adherent cells. This technique exploits the fact that mitotic cells downregulate adhesion molecules on the plasma membrane and become more spherical and loosely attached to culture surfaces (Suzuki et. al., 2003).

The caveat to all these methods of cell synchronization is the induction of cellular stress (metabolic, pharmacological, and mechanical) and the subsequent activation of stress responses that may confound the interpretation of results. Indeed, there is evidence that nocodazole induces the UPR, possibly by disrupting ER-microtubule associations and therefore the ER's structure (Seyb et. al., 2005).

Fluorescent reporters of cell cycle progression that allow tracking and separation of individual cells in different phases of the cell cycle without metabolic, pharmacological, or mechanical perturbations bypass the limitations that traditional methods of cell synchronization pose. The Fluorescent Ubiquitination-based Cell Cycle Indicator (FUCCI) system is a bi-cistronic reporter system that utilizes two cell cycle licensing proteins, CDT1

and Geminin, fused to red monomeric Kusibara-Orange2 (mKO2) and green monomeric Azami-Green (mAG) fluorescent proteins respectively (Figure 2). CDT1 is naturally degraded in S/G_2, and Geminin is degraded in G_1 (Benmaamar and Pagano 2005, Nishitani et. al., 2000, Vodermaier et al., 2004, Wei et. al., 2004). In this way, the FUCCI system identifies G_1 cells based on red fluorescence and S/G_2 cells based on green fluorescence (Sakaue-Sawano et. al., 2008).

The FUCCI reporter system has two main advantages that facilitate the cell biological and biochemical analyses of cells in different stages of the cell cycle. First it allows the physical separation of cells in G_1 and S/G_2 phases in an asynchronous population by fluorescence activated cell sorting (FACS). Second, the FUCCI system allows single cell analysis by live cell imaging.

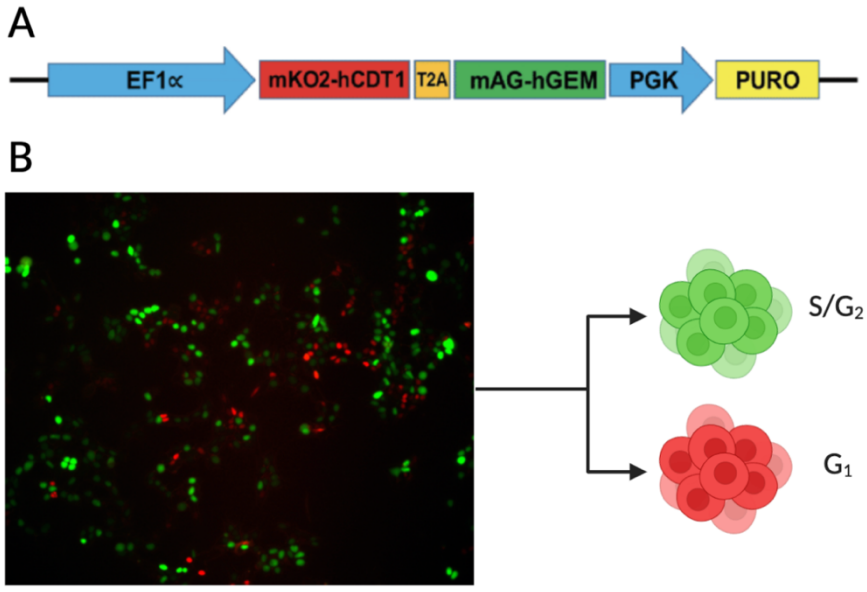

Fig 2. (A) Fast-FUCCI construct from Koh et. al., 2017. The human EF1α promoter controls the expression of a cell cycle licensing factors hCDT1 and hGEM fused to mKusibaraOrange2 and mAzamiGreen fluorophores respectively and separated by a T2A sequence. The human PGK promoter controls the expression of a puromycin resistance gene allowing for antibiotic selection of transduced cells. (B) Experimental Workflow: HEK-293T Fast-FUCCI cells before FACS. Cell cycle stages are physically separated by gating for red or green cells and are collected for biochemical analysis.

The experiments described in this thesis utilize a version of the FUCCI system, known as Fast-FUCCI, that combines both fusion protein reporters into a single polycistronic lentiviral vector separated by a T2A self-cleaving peptide that ensures an equimolar delivery of both reporter constructs (Koh et. al., 2017) (Figure 2). Introducing the Fast-FUCCI reporter into cells expressing the CRISPRi machinery consisting of a catalytically dead Cas9 protein fused to a transcriptional repressor (Gilbert et. al., 2013) allowed us to deplete genes of interest to dissect the contributions of the UPR in cell cycle progression. In this system, the catalytically dead Cas9 gene is appended to the KRAB (Krüppel associated box) domain of Kox1, and acts as a repressive chromatin modifier domain, further silencing gene expression.

CHAPTER 1

The ER volume and its chaperone and foldase content increases during interphase

We hypothesized that cells physically enlarge the ER and increase levels of ER foldases and chaperones in preparation for cell division. To test this hypothesis, we engineered H4 neuroglioma cells carrying the FUCCI reporter, separated them in G_1 or S/G_2 by fluorescence activated cell sorting (FACS), and measured their ER volume and chaperone and foldase content by electron microscopy and immunostaining, respectively. We analyzed the levels of the ER resident proteins BiP/HSPA5, Calnexin, and PDIA1 using Alexa488 conjugated secondary antibodies that emit in the far-red spectrum and therefore did not interfere with the FUCCI reporter fluorophores.

BiP, encoded by the gene HSPA5 is the most abundant ER chaperone and assists the folding of nascent polypeptides as they enter the ER lumen (Ni and Lee, 2007). BiP also plays a regulatory role in the fine tuning of the UPR as described above (Introduction, Section 3). BiP expression can be induced by either XBP1s or ATF6-N (Yamamoto et. al., 2004). Calnexin is a part of the protein folding quality control mechanism of the ER. Calnexin binding to misfolded N-linked glycoproteins retains them in the ER and allows more time to attempt re-folding (Koslov et. al., 2020). PDIA1 is a protein in a family of protein disulfide isomerases that catalyze disulfide bond rearrangement to ensure secretory proteins achieve the correct tertiary and quarternary structure (Parakh et. al., 2015).

After immunostaining, cells in G_1 (mKO2 positive) and G_2 (mAzamiGreen positive) were analyzed by flow cytometry to measure the levels of BiP/HSPA5, Calnexin, and PDIA1. Our unpublished findings showed an increase in the mean fluorescence intensity in G_2 cells

compared to G_1, indicating that the levels of BiP, Calnexin and PDIA1 increase in G_2 (Sabrina Solley MA thesis, Figure 14, UCSB, 2020). Similar analyses on Jurkat T-cell leukemia cells devoid of FUCCI reporters, corroborated these findings. In these experiments, I stained an asynchronous population of these cells with DAPI as well as with antibodies against the ER residents indicated above and analyzed the G_1 and G_2 phases using DNA content as a proxy for cell cycle stage (Figure 3). Analysis (by qRT-PCR) of H4 neuroglioma cells carrying the FUCCI reporter indicated an increase in the mRNA levels of these chaperones and foldases, further validating our findings. (Figure 4)

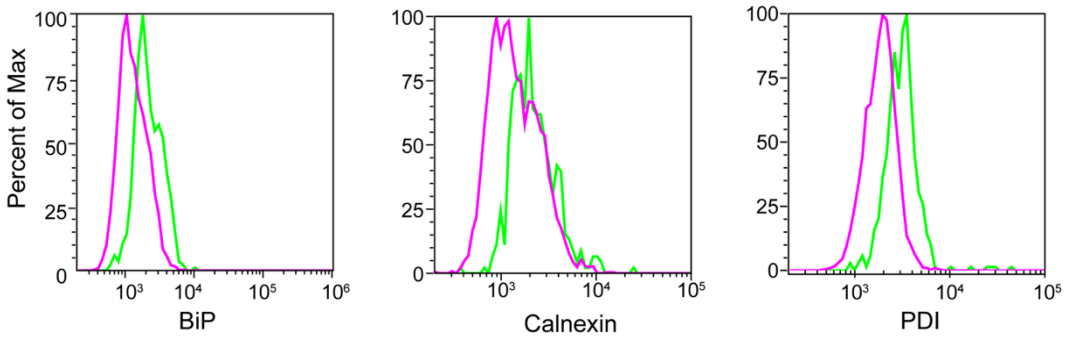

Fig 3. Jurkat-dCas9 cells were immunostained for ER chaperones and foldases and DNA stained with DAPI. Cells were gated into G_1 and G_2 stages based on DNA content, and the mean fluorescence intensity of the immunostaining was analyzed. G_1 cells (pink) show less ER chaperone and foldase content compared to G_2 cells (green). n = 3

One interpretation of the results above is that an increase in ER resident proteins is consistent with a concomitant increase in ER size (i.e., volumetric expansion) to allow more physical space for nascent peptides to fold in. However, it is also possible that the ER volume is not altered, and the influx of more foldases into the same volume increases the density of

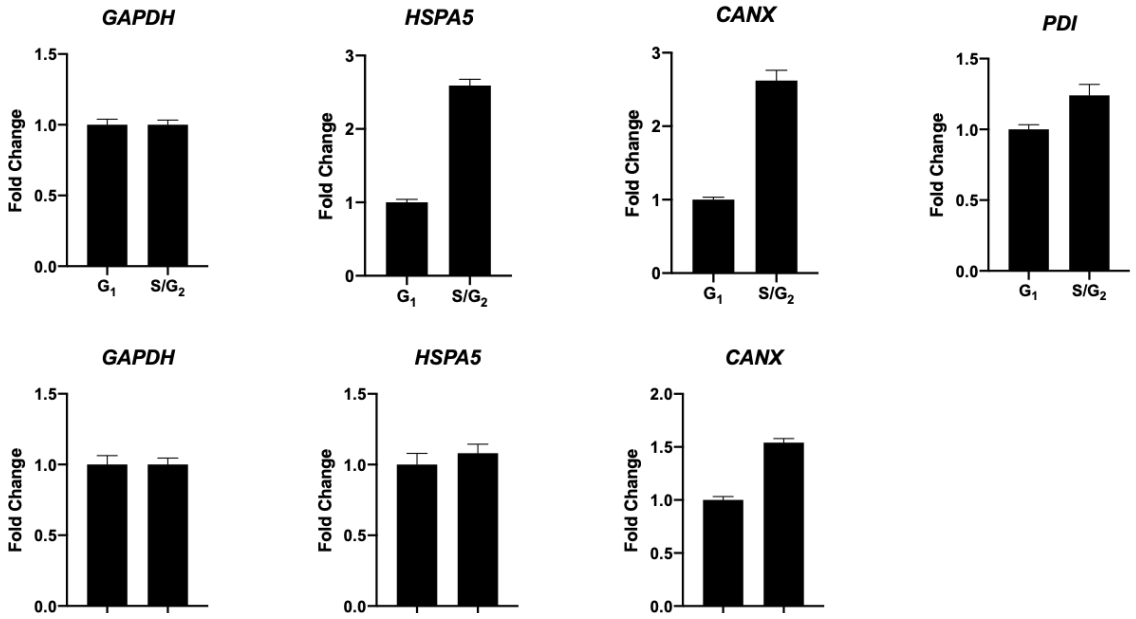

Fig 4. H4-dCas9 (top) and KMS11-dCas9 (bottom) FUCCI cells were sorted into G_1 or S/G_2 phases and RNA levels of ER resident chaperones and foldases in each phase were analyzed by qRT-PCR. Enrichment: S/G_2 compared to G_1. Error bars: SEM, n = 1

foldases available to nascent peptides, and therefore facilitates proper folding. To ascertain whether the ER volume actually changes during the cell cycle we measured the volume of the ER of FUCCI-carrying cells in G_1 or S/G_2 by transmission electron microscopy (Figure 5). In these experiments we observed a significant increase in ER volume in cells in S/G_2 when compared to cells in G_1 in two FUCCI cell lines, KMS11-dCas9 (multiple myeloma) and H4-dCas9 (neuroglioma), lending support to the notion that the volume of the ER expands during interphase.

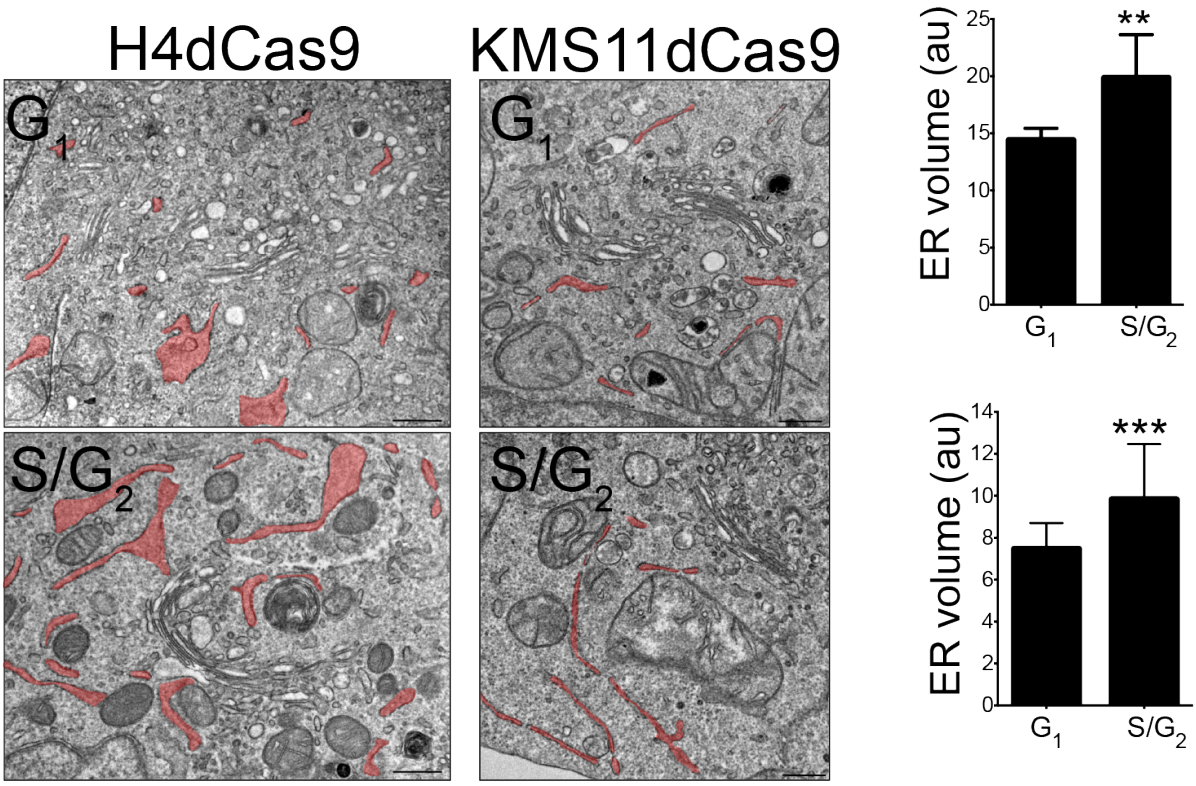

Fig 5. (Left) TEM analysis of H4-dCas9 and KMS11-dCas9 FUCCI cells reveals a significant increase in ER volume in G_2 cells as compared to G_1. (Right) Quantification of ER cisternal volume in H4-dCas9 FUCCI (Top), and KMS11-dCas9 FUCCI (Bottom). Error bars: SD, ** $p < 0.02$, **** $p < 0.005$

CHAPTER 2

The UPR activation threshold is different in G_1 and G_2

The results in Chapter 1 suggest that cells in G_1 and G_2 may have a differential sensitivity to disruptions of ER homeostasis. One scenario is that a large ER in S/G_2 cells buffers ER stress, by providing more physical space for nascent proteins to fold in, thus leading to higher ER stress tolerance and a higher threshold for activation of the UPR. A mutually exclusive scenario is that the ER expansion in S/G2 cells is accompanied by an increase in the UPR ER stress sensors (IRE1, PERK and ATF6), making these cells more efficient at inducing the UPR (i.e., lower UPR activation threshold and higher sensitivity to ER stress). To distinguish between these possibilities, I separated H4-dCas9 FUCCI cells into G_1 and S/G_2 by FACS and then treated each population with the N-linked glycosylation inhibitor tunicamycin at 2.5µg/mL for 4 hours, a classical ER stress-inducing agent. Analysis by qRT-PCR revealed that induction of UPR target genes from all three branches was enhanced in S/G_2 cells upon tunicamycin treatment compared to G_1 cells, supporting the latter scenario (Figure 6). Furthermore, levels of the UPR sensors were increased in S/G_2 cells compared to G_1 when analyzed by qPCR. (Figure 7)

This difference in sensitivity to ER stress was also evident in G_1 and G_2 cells in the absence of tunicamycin. I observed the same effect in HEK-293T FUCCI cells that also harbor bioluminescent reporters of *XBP1* and ATF4 activation, further substantiating the notion that G_2 cells are more sensitive to ER stress. (Figure 8) To discard any potential contributions of either the Fast-FUCCI system, or the process of cell sorting, to the differential ER stress sensitivity described above, I synchronized H4-dCas9 cells using thymidine (G_1) or thymidine

and nocodazole (G_2) and measured UPR activity upon tunicamycin treatment. This experiment substantiated the results obtained in FUCCI cells and indicated that the FUCCI reporter does not contribute to the differential ER stress sensitivity of G_1 and G_2 cells (Figure 9)

b

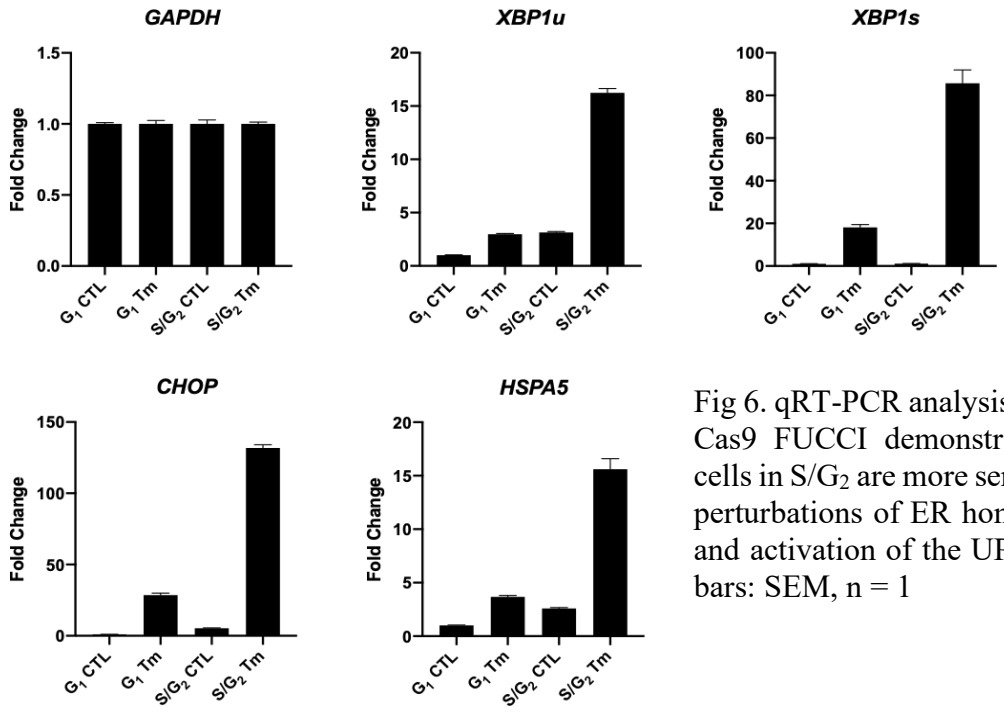

Fig 6. qRT-PCR analysis of H4d-Cas9 FUCCI demonstrates that cells in S/G_2 are more sensitive to perturbations of ER homeostasis and activation of the UPR. Error bars: SEM, n = 1

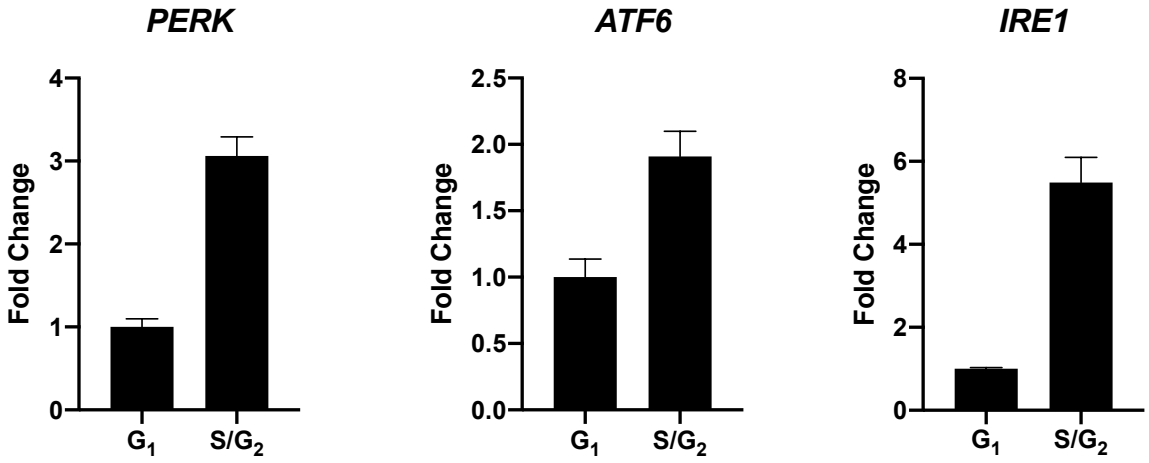

Fig 7. qRT-PCR analysis of H4-dCas9 FUCCI cells demonstrates that cells in S/G_2 have more UPR sensors than cells in G_1. Error bars: SEM, n = 1

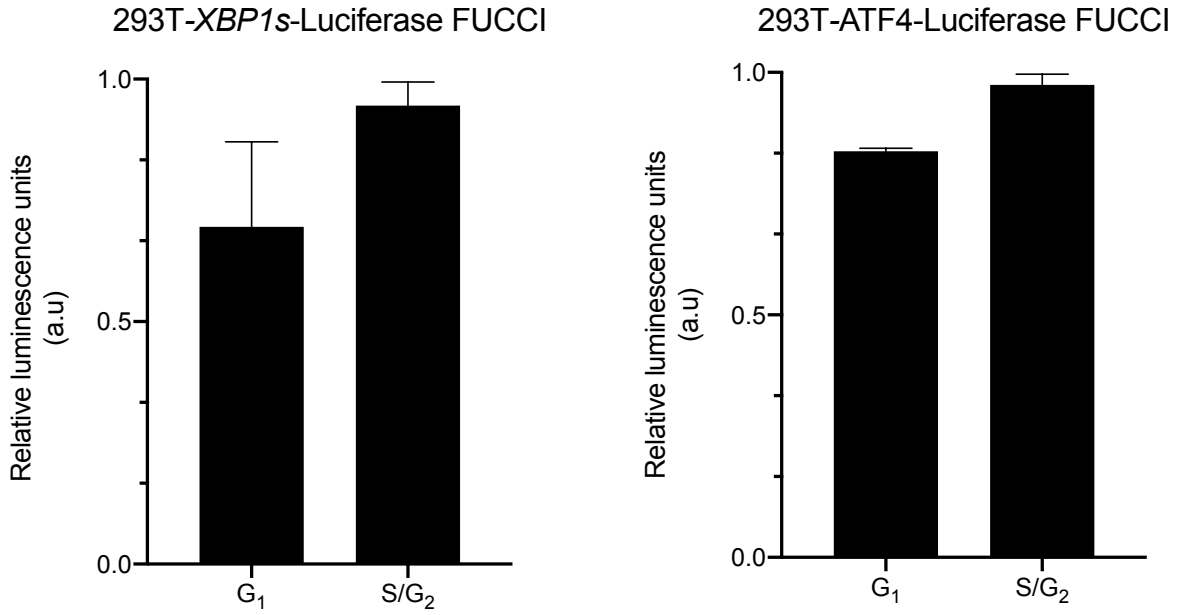

Fig 8. HEK-293T FUCCI cells harboring firefly luciferase reporter constructs that report on the splicing of the *XBP1* mRNA or the selective translation of the ATF4 uORF during ER stress were separated by FACS and the luminescence levels analyzed in the absence of ER stress. Increased luminescence was observed for both reporters in S/G_2 cells compared to G_1. Error bars: SD, n = 1

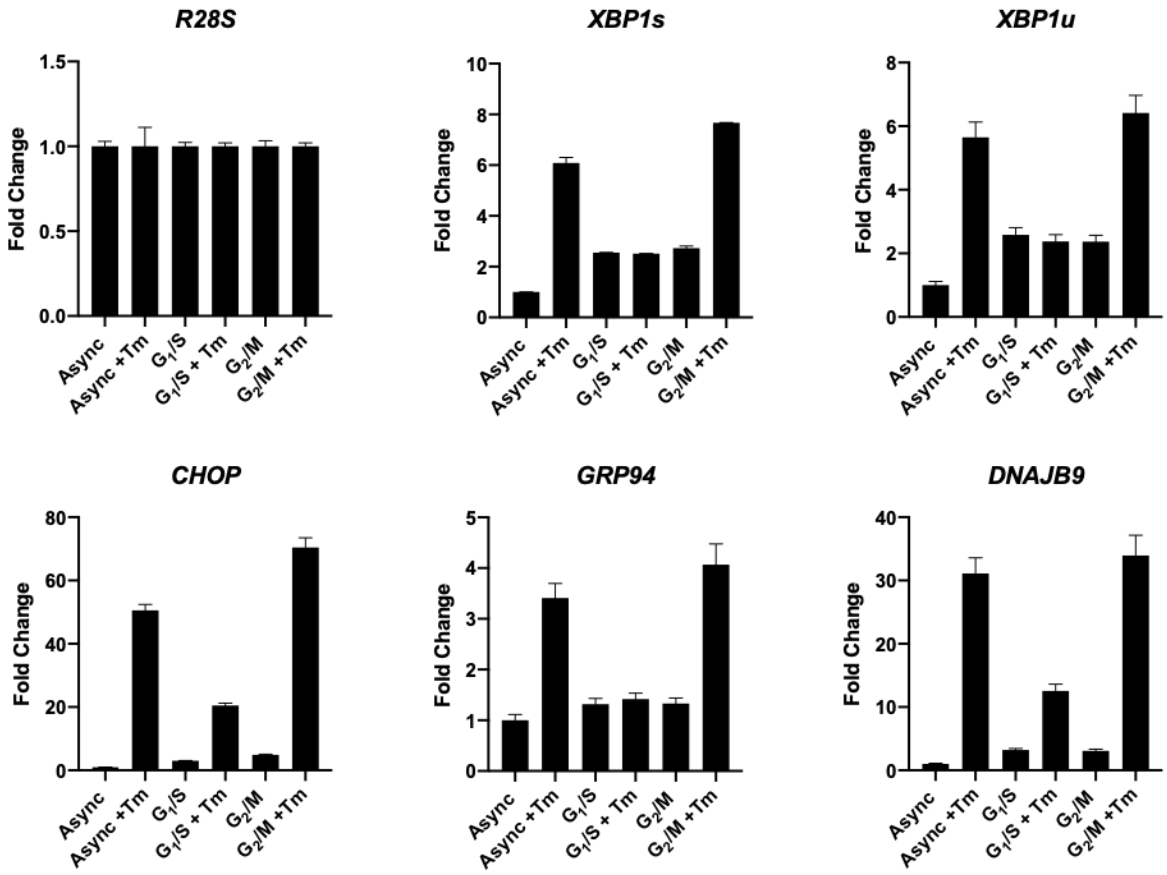

Fig 9. H4dCas9 cells were synchronized in G_1/S or G_2/M and treated with tunicamycin. Analysis of the indicated levels of mRNA expression by qRT-PCR of key genes shows that G_2/M cells are more sensitive to ER stress. Error bars, SEM, n = 1.

CHAPTER 3

UPR inhibition negatively impacts progression through the cell cycle

If the UPR plays a physiological role in the proper progression of the cell cycle, then it is reasonable that blocking the UPR should delay cell cycle progression. Cell cycle progression delays caused by inhibition of a single branch of the UPR could be small because of functional redundancy between the arms of the UPR. Indeed, pharmacological inhibition of single UPR arms showed modest cell cycle delays with acute exposure to the UPR inhibitors (Figure 10, days 0-5). I reasoned that culturing cells over longer periods (16 days, which corresponds to over 10 generations) in the presence of pharmacological inhibitors of the UPR would reveal cell cycle delays. In these experiments I used 4μ8C (at 10μM) to block IRE1's RNase activity, ISRIB to bypass the phosphorylation of eIF2α induced by PERK (at 500nM), and ceapin A7 (at 5uM) to inhibit the proteolytic processing of ATF6, which were freshly supplemented at each media exchange to ensure chronic UPR blockade.

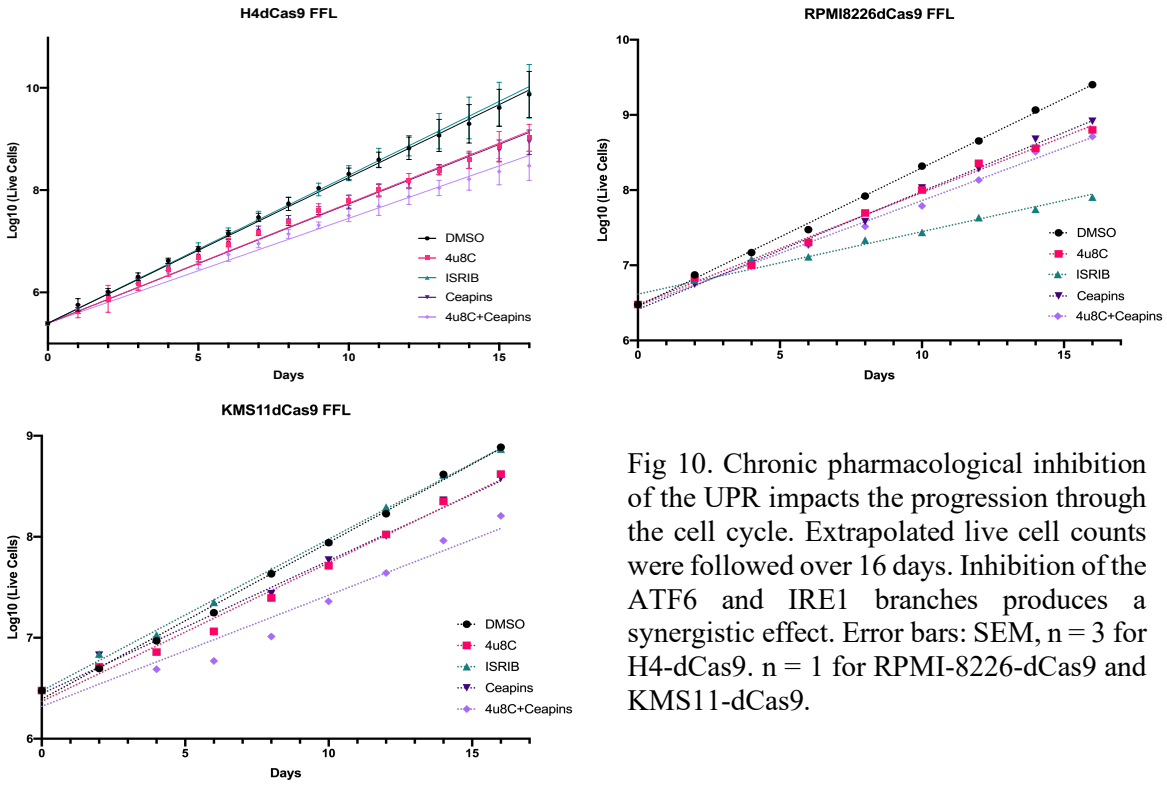

Fig 10. Chronic pharmacological inhibition of the UPR impacts the progression through the cell cycle. Extrapolated live cell counts were followed over 16 days. Inhibition of the ATF6 and IRE1 branches produces a synergistic effect. Error bars: SEM, n = 3 for H4-dCas9. n = 1 for RPMI-8226-dCas9 and KMS11-dCas9.

It is important to note that all of these pharmacological inhibitors are established molecules with no chronic toxicity effects reported. (Gallagher et. al., 2016, Cross et. al., 2012) While ISRIB showed no effect in proliferation rate compared to the control treatment in KMS11-dCas9 and H4-dCas9 cells, RPMI-8226-dCas9 (multiple myeloma), cells treated with ISRIB proliferated much slower than in any other treatment including the control treatment. One possible explanation for this discrepancy in the effect of ISRIB is the secretory burden of different cell lines. It is possible that the biosynthetic capacity of RPMI-8226-dCas9 has approached its maximum, and ISRIB-mediated enhancement of protein synthesis would push the cells over the limit. By contrast, inhibition of IRE1 and ATF6 slowed cell proliferation in all cell lines when compared to the control treatment. Co-administration of 4μ8C and ceapin A7 showed a synergistic effect and slowed down cell proliferation to a greater extent.

To rule out potential off-target effects of the pharmacological UPR inhibitors, I corroborated the results by genetic depletion of each UPR sensor using CRISPRi (Figure 11). In these experiments, I labelled UPR KD cells with eGFP and a GAL4 (non-targeting sgRNA) control cell line with mCherry. I combined these cells in equal proportions (for each branch of the UPR) to establish competition assays in co-culture. If UPR KD cells show a proliferative disadvantage, as suggested by my experiments with pharmacological UPR inhibitors, the mCherry+ cells would be expected to take over the culture over time. I collected samples every 48 hours in 16-day competition assays to analyze the proportions of eGFP+ and mCherry+ cells by flow cytometry. The PERK KD cells showed the largest overall proliferative disadvantage (5:1 control to KD at day 16), followed by ATF6 KD cells (5:2 control to KD at day 16), and IRE1 KD cells (5:3 control to KD at day 16). Taken together, these experiments

corroborated that inhibition of all UPR branches conferred a proliferative disadvantage (Figure 11, Figure 12).

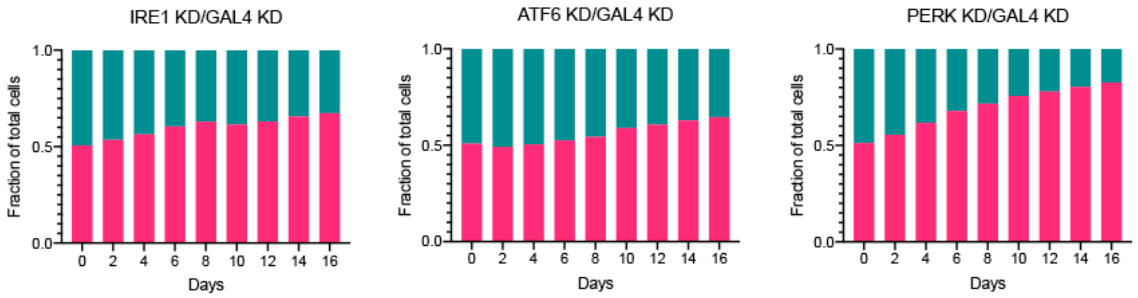

Fig 11. H4-dCas9 CRISPRi cell lines lacking the three UPR sensors and labeled with eGFP were cocultured with mCherry labeled H4-dCas9 cells expressing a non-targeting GAL4 sgRNA. Cells were harvested every two days for analysis by flow cytometry, and the proportion of eGFP+ and mCherry+ cells were assessed over a period of 16 days. n = 3

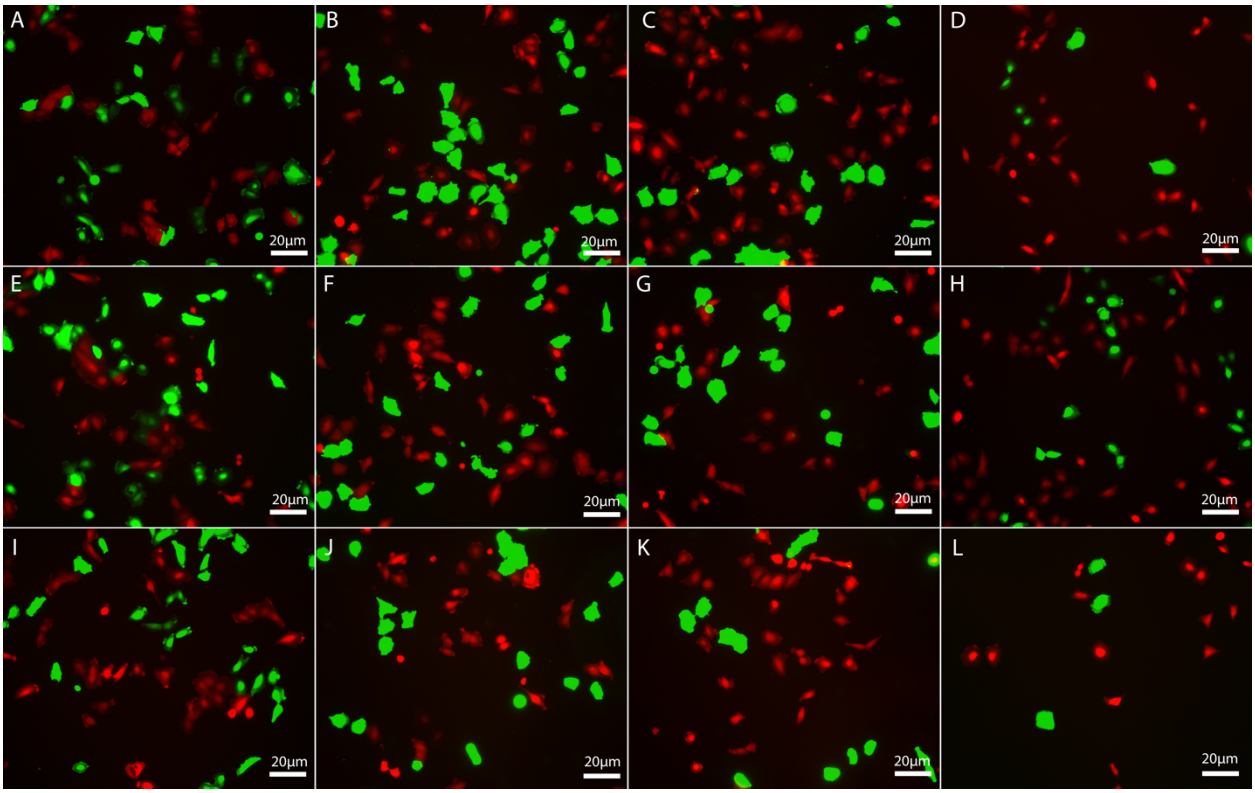

Fig 12. UPR KD/Gal4 KD coculture populations labeled with EGFP and mCherry respectively. (A-D) ATF6 KD/Gal4 KD (E-H) IRE1 KD/Gal4 KD (I-L) PERK KD/Gal4 KD. Left to right, panels depict the populations at Day 1, Day 5, Day 9, and Day 15.

CHAPTER 4

The G_2/M cell cycle checkpoint kinase PKMYT1 modulates the UPR

Unpublished data from our lab suggests regulatory crosstalk between the UPR sensor IRE1 and the G_2/M checkpoint kinase PKMYT1. These experiments demonstrated that the IRE1 inhibitor, 4μ8C, antagonized the negative effects on cell viability produced by pharmacological inhibition of PKMYT1 (Figure 13; Acosta-Alvear, unpublished).

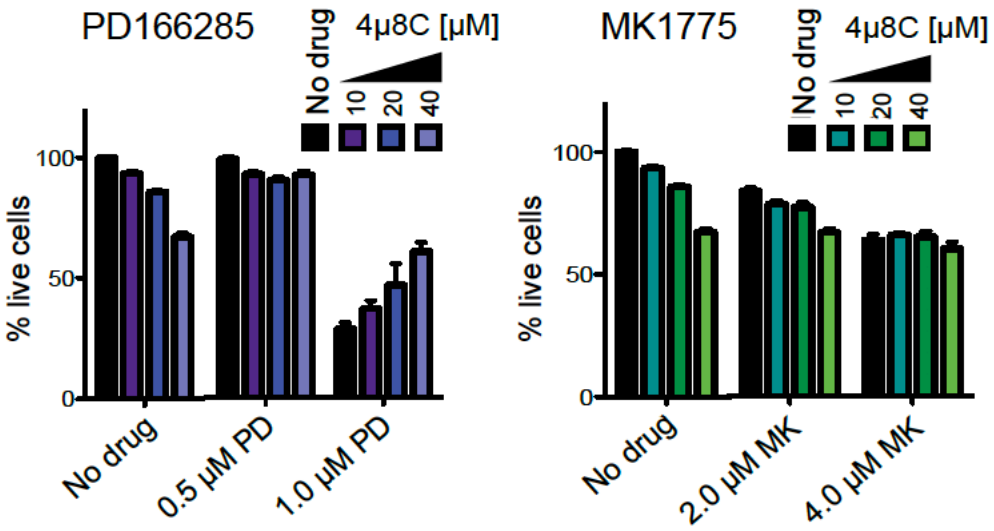

Fig 13. Treatment with the IRE1 inhibitor 4μ8C rescues the decrease in cell viability observed upon treatment with the PKMYT1 inhibitor PD166285. Note that the effect is specific to PD166285and not observed upon blocking PKMYT1's sister kinase WEE1 with the WEE1 pharmacological inhibitor MK1775 Error bars: SD, n = 3

Forced expression of PKMYT1 dampened IRE1 signaling (Figures 14, 15) while knockdown of PKMYT1 enhanced it, lending support to the notion that that PKMYT1 negatively regulates IRE1. (Figures 16, 17). In these experiments, I used a doxycycline-inducible PKMYT1-eGFP construct stably expressed in U2OS-dCas9 cells to force expression of PKMYT1 and, in

parallel, introduced sgRNAs targeting endogenous PKMYT1 to knock it down, respectively. In agreement with my hypothesis, *XBP1* splicing (as measured by qRT-PCR) was also diminished upon forced expression of PKMYT1 (Figure 14). Although the semi-quantitative PCR did not exactly corroborate this result, the higher precision of qRT-PCR as a technique suggests a technical artifact with the gel result (Lower right panel, Figure 14). Notably, forced expression of PKMYT1 not only muted IRE1 signaling but also PERK and ATF6 signaling, as evidenced by CHOP and GRP94 mRNA levels (measured by qRT-PCR), which serve as proxies for their respective induction upon tunicamycin treatment.

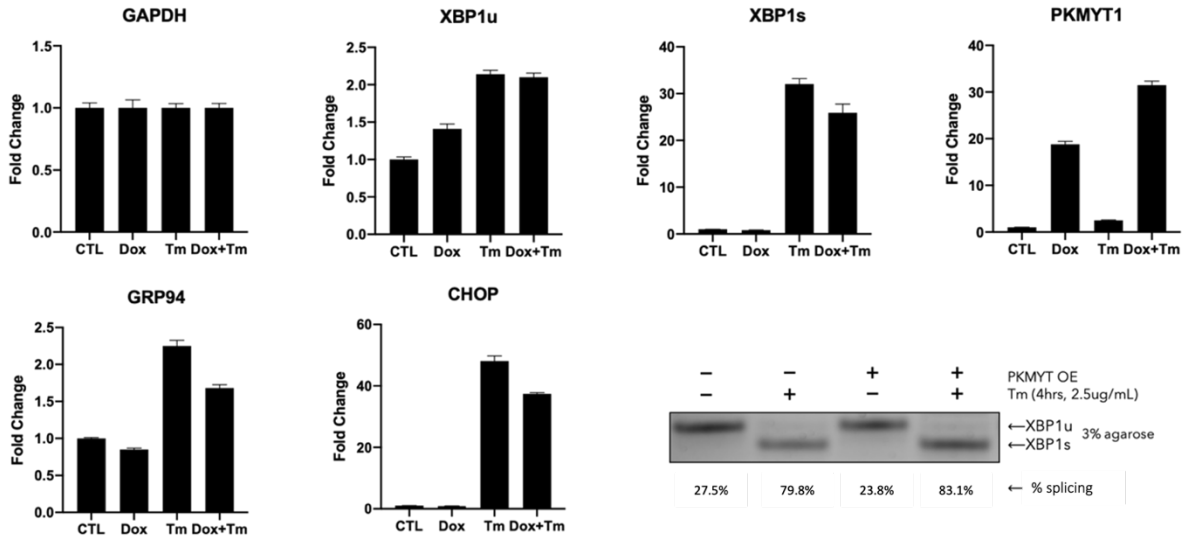

Fig 14. U2OS-dCas9 cells harboring a doxycycline inducible PKMYT1-eGFP construct were induced for 24 h with doxycycline before treatment with tunicamycin for 4 h. Analysis by qRT-PCR demonstrates that UPR signaling is dampened in the population overexpressing PKMYT1. Error bars: SEM, n = 3. (Bottom right) Semi quantitative PCR using primers that amplify both *XBP1u* and *XBP1s* from cDNA, separated on 3% agarose. Lower band is the spliced isoform. Quantification indicates the proportion of XBP1s to the total XBP1 content expressed as % splicing

In line with the results above, forced expression of PKMYT1 also dampened the response of *XBP1s* and ATF4 luciferase reporters in cells treated with tunicamycin, further strengthening the conclusion that PKMYT1 negatively regulates the UPR (Figure 15)

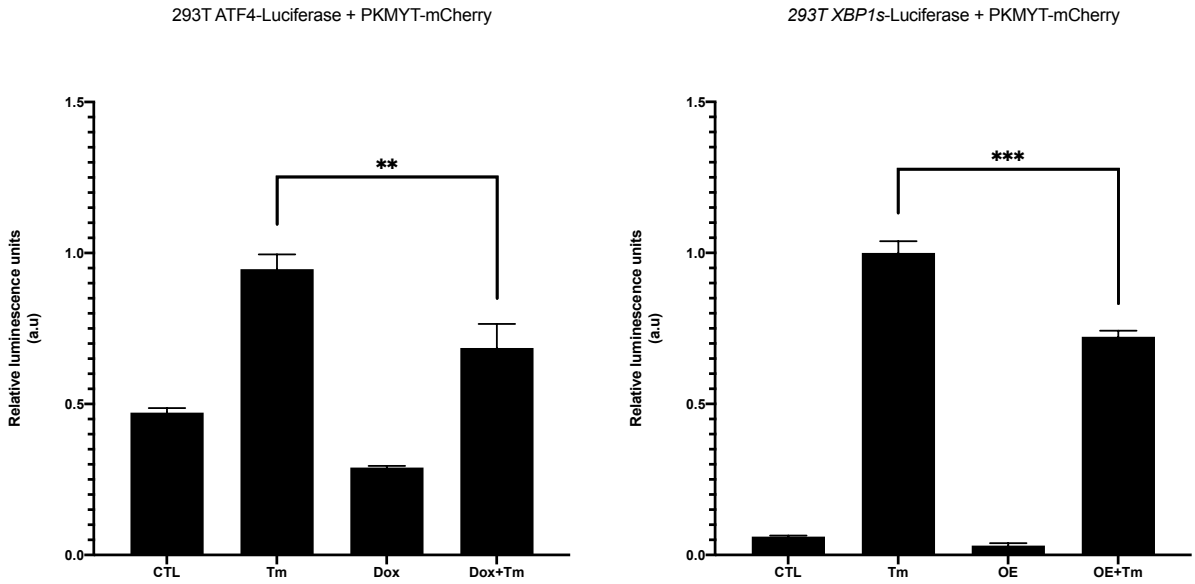

Fig 15. (Left) A stable HEK-293T-ATF4 luciferase reporter cell line harboring a doxycycline inducible PKMYT1-mCherry construct was pretreated with doxycycline for 24 h and then treated with tunicamycin for 6 h. (Right) A HEK-293T- XBP1s luciferase reporter cell line was transfected with an eGFP-PKMYT1 construct to overexpress PKMYT1 prior to treatment with tunicamycin for 6 h. In both cases, overexpression dampened the luminescence signal from the reporters, indicating a negatively modulatory effect of PKMYT1 on UPR signaling. Error bars = SD, n = 3, ** p = 0.0084, *** p = 0.0004.

The reciprocal experiment in which I depleted PKMYT1 in H4-dCas9 and U2OS-dCas9 cells using CRISPRi and treated the cells with tunicamycin showed the expected opposite phenotype: enhanced signaling from all three UPR branches (Figures 16, 17), further substantiating that that PKMYT1 acts a negative UPR regulator.

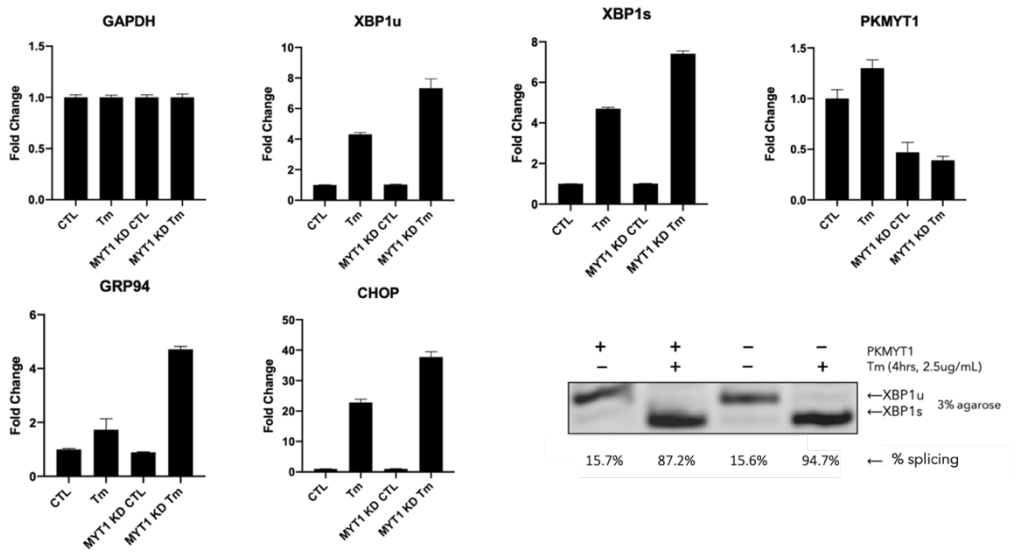

Fig 16. H4-dCas9 cells depleted of PKMYT1 were treated with tunicamycin. Analysis by qRT-PCR demonstrates that UPR signaling from all three branches is enhanced in the population lacking PKMYT1. Error bars: SEM, n = 1. (Bottom right) Semi quantitative PCR using primers that amplify both *XBP1u* and *XBP1s* from cDNA, separated on 3% agarose. Lower band is the spliced isoform. Quantification indicates the proportion of XBP1s to the total XBP1 content expressed as % splicing

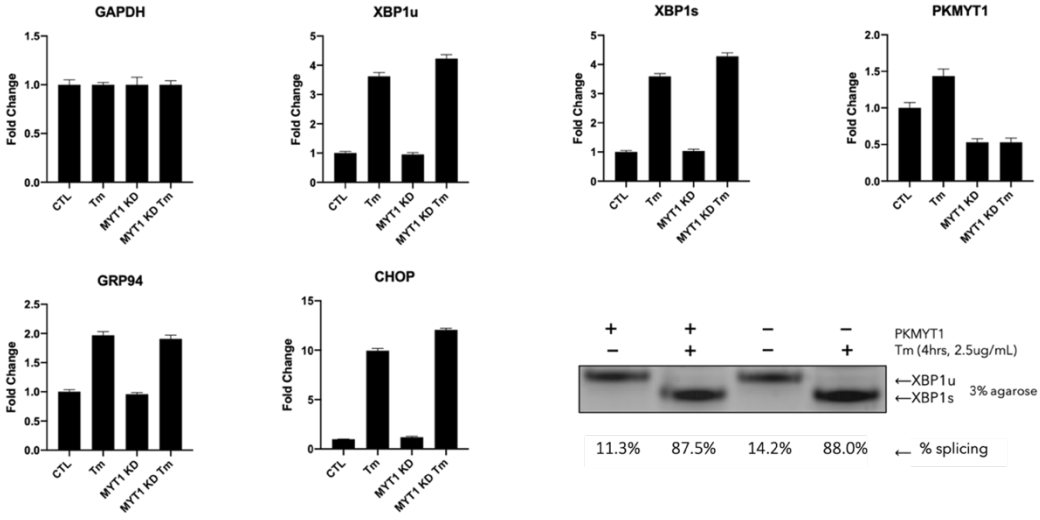

Fig 17. U2OS-dCas9 cells depleted of PKMYT1 were treated with tunicamycin. Analysis by qRT-PCR demonstrates that UPR signaling from all three branches is enhanced in the population lacking PKMYT1. Error bars: SEM, n = 1. (Bottom right) Semi quantitative PCR using primers that amplify both *XBP1u* and *XBP1s* from cDNA, separated on 3% agarose. Lower band is the spliced isoform. Quantification indicates the proportion of XBP1s to the total XBP1 content expressed as % splicing

PKMYT1 could negatively regulate the UPR directly or indirectly: through physical association and modulation of the functions of UPR sensors, or by inducing responses that impact UPR activity. To ascertain whether PKMYT1 interacts with UPR sensors, I force expressed fluorescently labelled PKMYT1-mCherry in the background of a U2OS cell line null for IRE1α (CRISPR KO), that also carries a doxycycline-inducible fluorescently labelled IRE1 transgene (IRE1-mNeon) (Belyy et. al., 2021). Since PKMYT1-mCherry is also under the control of a doxycycline-inducible promoter, this experimental setup allows the concurrent forced expression of both fluorescently labelled proteins.

Preliminary live-cell confocal microscopy analysis of the cells expressing IRE1-mNeon and PKMYT1-mCherry revealed that a subset of PKMYT1 colocalized with a subset of IRE1 in punctate structures in the absence of stress (Figure 18). IRE1 puncta are observed during the UPR and are classically thought to be the sites of IRE1 activation (Belyy et. al., 2021). However, recent studies investigating the signaling dynamics of IRE1 suggest that IRE1 clusters in fact exclude its most well characterized target, the *XBP1* mRNA. This suggests that IRE1 clusters may be a way to buffer the overactivation of the UPR by way of sequestering inactive IRE1 molecules. (Goméz-Puerta et al., 2021) Other studies from our lab presented similar findings about the signaling dynamics of PKR (a kinase in the Integrated Stress Response) in which PKR clusters exclude its best characterized enzymatic target eIF2α, suggesting that clustering may be a universal mechanism for buffering signal output (Zappa et. al., 2021).

Indeed, the colocalization of IRE1 and PKMYT1 was lost upon treatment with tunicamycin, although IRE1 puncta were still present (Data not shown) This result suggests that PKMYT1 could potentially interact with IRE1 at steady state to prevent spurious

activation in the absence of stress. More rigorous mechanistic analyses are required to understand the role of PKMYT1 in modulating the UPR. While our data suggest that PKMYT1 may associate with IRE1, additional experiments are required to ascertain whether this interaction is a real biological phenomenon rather than a technical artifact and whether PKMYT1 may also associate with PERK and ATF6.

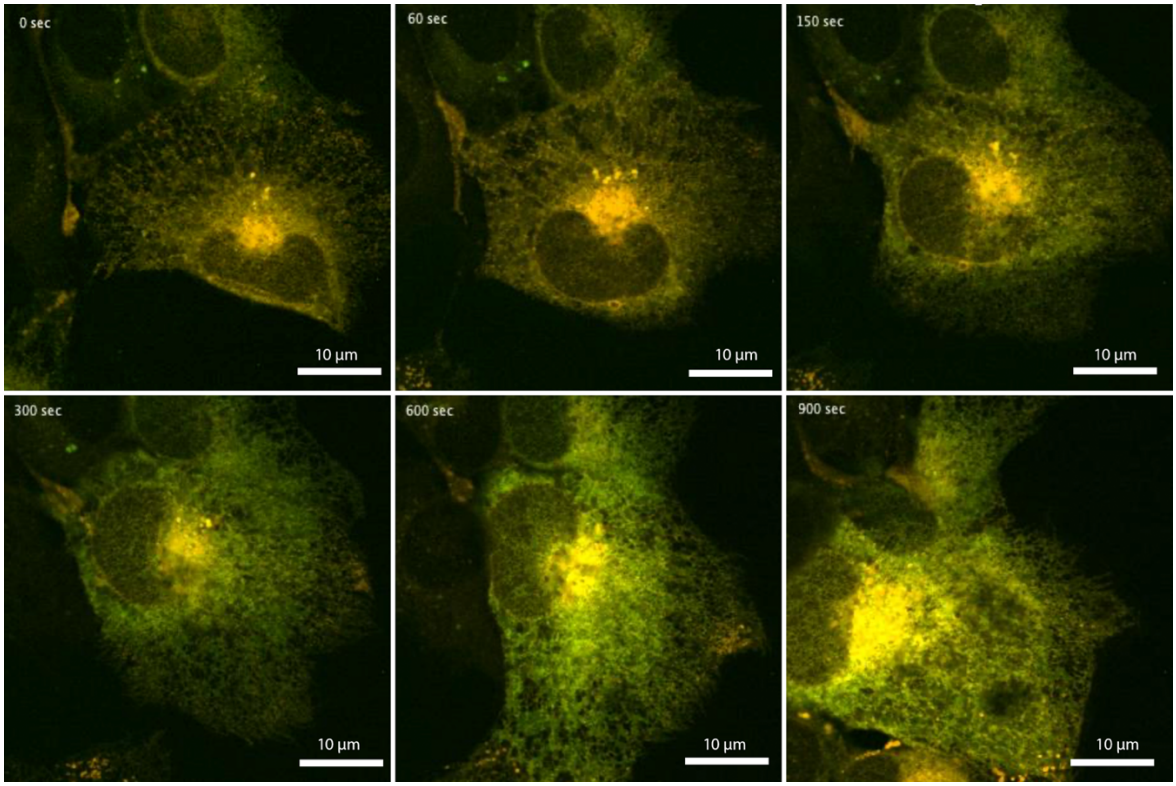

Fig 18. U2OS-dCas9 cells overexpressing IRE1-mNEON and PKMYT1-mCherry. The ER localization of IRE1 and the Golgi localization of PKMYT1 is readily observable at 0s. A subset of IRE1 and PKMYT1 signals overlap, resulting in a yellow fluorescent signal. Cells were imaged using spinning disc confocal microscopy, over a period of 6 h.

CHAPTER 5

Future Directions

Further experiments are required to uncover the reason for the lowered threshold of UPR activation in S/G_2 cells, but there are several possible explanations. First, although the increased volume and chaperone content in S/G_2 FUCCI cells suggest that ER folding capacity is greater in S/G_2 cells, it is possible that global translation in S/G_2 cells is also increased compared to G_1. Such a scenario could favor a potential increase in unfolded proteins entering the ER and triggering the UPR upon the disruption of the protein folding environment of the ER. Second, since membrane expansion occurs over the course of the cell cycle, the increase in ER volume in S/G_2 cells may be coupled with a change in ER membrane composition that activates the UPR sensors independent of protein folding load. A third possibility is that the architecture of the ER is remodeled in S/G_2 cells such that hubs of protein folding exist in subdomains of the ER where the UPR sensors are enriched. Since this phase is a critical stage prior to mitotic entry, an organizational ER subdomain might allow for small defects in protein folding to be recognized and corrected by the UPR. Indeed, ER signaling subdomains have been an attractive idea for many years in the field, and there is emerging evidence that they may actually play an important role in organizing and functionalizing the ER (Hetz et. al. 2020)

By sorting G_1 and S/G_2 FUCCI cells and incorporating a chain terminator tRNA mimetic such as puromycin, peptides that are actively being translated can be detected by western blotting using antibodies against puromycin to assess levels of global translation. However, there is the possibility that the differences in global protein translation between the two stages are too small to detect by western blot in which case approaches such as following

the incorporation of ^{35}S-cysteine into nascent proteins may prove to be more useful. An IRE1 mutant lacking the ER lumenal sensor domain expressed in the background of endogenous IRE1 deletion would allow to decouple the protein folding load of the ER from IRE1 activation by ER lipid bilayer stress. By synchronizing this cell line to either G_1/S using a double thymidine block or to G_2/M using thymidine/nocodazole block and assessing levels of *XBP1* splicing and its target genes, we can potentially unravel the contribution of lipid composition versus protein loading to the lowered threshold for UPR activation in the two stages of the cell cycle.

It is noteworthy that PKMYT1— a G_2/M checkpoint kinase that is active during G_2— is a potential negative regulator of the UPR, especially in light of our results showing that cells in G_2 are more proficient at activating the UPR (see Chapter 2). This paradox could be explained by the inactivation of PKMYT1 during checkpoint recovery. PKMYT1 activity is tightly coupled to the G_2/M checkpoint, with CDK1 and Plk1 both playing roles in the inactivation of PKMYT1 during checkpoint recovery through phosphorylation. PKMYT1 is activated at the checkpoint, and then inactivated during checkpoint recovery. Since our methods to study the G_2 population synchronize the cells at the G_2/M checkpoint, the bulk of the cells are expected to transition out of the checkpoint blockade. It is therefore possible that the heightened sensitivity to ER stress *follows* the inactivation of PKMYT1 at the G_2/M checkpoint recovery. Future experiments in synchronized, or FUCCI-selected cells depleted of PKMYT1 would allow testing this possibility.

Further studies are also required to determine whether PKMYT1 and IRE1 are indeed physically interacting. While early co-immunoprecipitations did not suggest a physical interaction, it is possible that the interaction is too transient or weak to capture by a simple co-

immunoprecipitation, but instead requires a crosslinked immunoprecipitation approach. Proximity labeling pulldown techniques could also be informative in this context and starting from a cell population that is synchronized to G_2 (the phase in which the interaction is likely to occur) will likely boost the probability of capturing a *bona-fide* interaction. Furthermore, since any interactions between IRE1 and PKMYT1 may be highly transient, a high-resolution time-lapse microscopy approach could be informative: with a split GFP pair, dynamic interactions could be tracked with much greater precision. It is interesting to speculate about the ways in which PKMYT1 may interact with one or more of the UPR sensors: further work will hopefully elaborate on the nature of these interactions and whether there are factors responsible for mediating those contacts.

Methods

1. Cell Culture

KMS11-dCas9-KRAB, RPMI-8226-dCas9-KRAB, and H4-dCas9-KRAB cells were a kind gift from Dr. Martin Kampmann (UCSF). HEK-293METR cells used for lentivirus packaging were a kind gift from Dr. Brian Rabinovich (formerly at MD Anderson Cancer Center). U2OS IRE1 KO IRE1-mNeon cells were a kind gift of Dr. Peter Walter (UCSF). KMS11 and RPMI-8226 cells were cultured in RPMI 1640 medium supplemented with 10% fetal bovine serum, 0.1 U/mL penicillin and 0.1 U/mL streptomycin, and 2mM L-glutamine. H4, U2OS, HEK-293METR, and HEK-293T cells were cultured in DMEM supplemented with 11mg/L sodium pyruvate, 10% fetal bovine serum, 0.1 U/mL penicillin, 0.1 U/mL streptomycin, and 2mM L-glutamine. All cell lines were maintained at 37°C with 5% CO_2 in a humidified incubator. All cell line derivatives were cultured identically.

2. Packaging and transduction of VSV-G pseudotyped lentiviral particles

HEK-293METR cells were grown to 60-70% confluence and transfected with the lentivector, and pVSV-G and pCMVΔR8.91 helper plasmids using Lipofectamine 2000 (Invitrogen), following the manufacturer's recommendations. The transfection mixture was replaced 24 h after transfection with virus collection media (DMEM supplemented with 11mg/L sodium pyruvate, 4% FBS, 0.1 U/mL penicillin, 0.1 U/mL streptomycin, 2mM L-glutamine, and 15mM HEPES at pH 7.5). Viral supernatants were collected 48 h after transfection and filtered through a 0.45um filter to remove cell debris. The filtered supernatant was concentrated approximately 5-fold using a centrifugal filter unit with a 100k MW cut-off.

The concentrated viral filtrate was used to infect target cells by spinoculation. Three days after infection, cells were selected with antibiotics or further expanded for FACS-based selection.

3. Fluorescence Activated Cell Sorting (FACS)

G_1 and S/G_2 FUCCI cell populations were selected by FACS. Cells expressing low levels of the FUCCI construct were separated from the rest of the cell population by gating on eGFP (AzamiGreen) positive cells that were also negative for mCherry (KusibaraOrange) to avoid selecting for cells expressing both fluorophores at the same time. Sorted cells were collected by centrifugation at 160 *x* g and resuspended in their respective growth media and recovered in the incubator for an hour prior to any drug treatments or analysis. The green and red lasers had an excitation/emission of 488/509 and 587/610 respectively. All FACS experiments were conducted in a Sony SH800S FACS instrument.

4. Cell Synchronization

Cells were grown to a confluence of approximately 50-60% prior to treatment with 2.5 mM thymidine for 16 h to synchronize the population at the G_1/S boundary. The following day, the cells were washed in PBS and allowed to recover for 8 h before exposing them for an additional 16 h to either 2.5 mM thymidine to synchronize the population at the G_1/S boundary, or with nocodazole (100 ng/mL for HEK-293T cell lines and derivatives, 300 ng/mL for all other cell types) to synchronize them at the G_2/M checkpoint. The initial treatment of thymidine followed by nocodazole allows the entire population of cells to synchronously transition to G_2 upon nocodazole treatment.

5. Cell fixation and staining for flow cytometry

Live cells were collected by centrifugation at 1.5 *x g*. The cell pellet was washed thrice in PBS to remove any residual cell culture media and resuspended in either 100 μL of PBS for ethanol fixation or 200 μL PBS for paraformaldehyde fixation. 350 μL of chilled 100% ethanol or 200 μL of 4% paraformaldehyde solution in PBS were added dropwise while vortexing the cell suspension gently. The cells were fixed at 4°C with gentle agitation for 15 minutes and recovered by centrifugation at 5 *x g* for 5 min prior to three washes with PBS to remove residual fixatives. The fixed cells were stored at 4°C until processing for flow cytometry analysis. Immediately before the flow cytometry analysis, the fixed cells were resuspended in PBS and incubated with 50 μg/mL propidium iodide and 100 μg/mL RNaseA for 15 minutes. For immunostaining, the fixed cells were resuspended in 200 μL of blocking and permeabilization buffer (50 mM NH_4Cl, 0.5% BSA, 0.05% saponin, 0.02% NaN_3 in PBS) and incubated at room temperature for 1 h. After blocking, the cells were resuspended in 50 μL of primary antibody at a 1:500 dilution and incubated overnight at 4°C with gentle agitation. The following day, the cells were resuspended in 50 μL of fluorophore conjugated secondary antibody (1:500 in blocking buffer) and incubated at room temperature for 1 h. Last, the cells were washed thrice in PBS and resuspended in 250 μL of PBS for flow cytometry analysis (see Materials for antibody details).

6. RNA extraction, cDNA synthesis, and qRT-PCR

5 x 10^5 to 2 x 10^6 cells were lysed in either Trizol reagent (ThermoFisher) or Buffer RLT (Qiagen) supplemented with 1% 2-mercaptoethanol and RNA was extracted according to the manufacturers' protocol. 1 μg of RNA was DNase treated with DNaseI (New England

Biolabs) according to the manufacturer's protocol, and cDNA was synthesized using the iScript cDNA synthesis system (BioRad) according to the manufacturer's protocol. The cDNA was diluted 10-fold in nuclease-free water and stored at -80 °C until use. Gene-specific quantitative PCR (qRT-PCR) on the template cDNAs was carried out using the SYBR Green Select Master Mix (ThermoFisher) according to the manufacturer's protocol. qRT-PCRs were carried out in a BioRad CFX96 Touch qPCR instrument. The Cq values were determined using regression fitting on the CFX Maestro software. Changes in gene expression were analyzed using the ΔΔCq method. Semi quantitative PCRs were performed using cDNA templates, Taq Polymerase (NEB), and the same primers as for qRT-PCR (see Materials). Reactions were separated on TAE agarose gels.

7. Microscopy

Images in Figure 5 were acquired by transmission electron microscopy. Briefly, 150-200 nM sections were obtained using a Leica Ultracut-UCT microtome, transferred onto copper slot grids, stained with Reynold's lead citrate, and imaged in a Tecnai 12 electron microscope set at 120 keV. ER surfaces were rendered with the IMOD software. Images in Figure 11 were acquired on an Echo Revolve microscope. Images in Figure 17 were acquired using an inverted spinning disc confocal microscope (Nikon Ti-Eclipse) equipped with an electron multiplying charge-coupled device camera (Fusion, SN:500241) and environmental control (Okolabs stage top incubator). Live cell imaging was performed at 37°C and 5% CO_2. Image acquisition was performed with a 40X NA 0.095 air objective.

8. Luciferase Assays

HEK-293T cells harboring either the *XBP1s* or ATF4 luciferase reporter constructs were seeded in white 96-well plates at a density of 20,000 cells per well. After incubation in media supplemented with 2.5 ug/mL tunicamycin for 4 hours, 50 μL of OneGlo Luciferase reagent (Promega) were added to each well and the plates were analyzed using a Wallac1420 plate reader.

9. Chronic UPR inhibition growth curves

Pre-sorted, low expressing FUCCI cell lines (H4-dCas9, KMS11-dCas9, and RPMI-8226-dCas9) were treated with UPR inhibitors (5 μM ceapin A7, 500 nM ISRIB, and 10 μM 4μ8C) over a period of 16 days with media and drug replacements every other day. H4-dCas9 cells were seeded at a density of 2.5 x 10^5 cells per well. KMS11-dCas9 and RPMI-8226-dCas9 cells were seeded at a density of 3 x 10^6 cells per plate. H4 cells were counted every day whereas KMS11 and RPMI-8226 cells were counted every other day. Each sample was counted twice at the subculture intervals indicated using Trypan Blue and an automated cell counter (Countess II FL, ThermoFisher). The numbers of live cells per unit volume at each time point were used to extrapolate the overall growth of the whole population over time.

10. Statistical Analysis

Wherever indicated, "n" refers to the number of biological replicates in an experiment. A Students T-test was used where possible, only for experiments with $n = 3$, to determine the statistical significance of the results. Statistical analysis was not performed for experiments with $n < 3$.

Materials

1. Primers for qPCR

Primer Name	5'-3' Primer Sequence
HSPA5	TGCAGCAGGACATCAAGTTC
	AGTTCCAGCGTCTTTGGTTG
CANX	TCAACCGGATGTGAAGGAA
	CACTCTCTTCGTGGCTTTCTG
CHOP	TTAAGTCTAAGGCACTGAGCGTATC
	TGCTTTCAGGTGTGGTGATG
DNAJB9	CGGATGCTGAAGCAAAATTC
	TTCTTGGATCCAGTGTTTTGG
GAPDH	AGCCACATCGCTCAGACAC
	TGGAAGATGGTGATGGGATT
GRP94	TCCAATTCAAGGTAATCAGAT
	CCAGTTTGGTGTCGGTTTCT
PDIA3	GACAACTTCGAGAGTCGCATC
	CACCTGCTTCTTCACCATCTC
PKMYT1	CCTGGTGCACCTTGATGTC
	ATGCCACTTCCAGGATGGT
R28S	CTTACCAAAAGTGGCCCACTA
	AAACTCTGGTGGAGGTCCGT
XBP1s exon 5	AATCGAGGAAGCACCTCTCA
	AAGCATCCAGTAGGCAGGAA
XBP1u exon 5	GTTGGGCATTCTGGACAACT
	TTCCAGCTTGGCTGATGAC
XBP1 total	GACATCCAGCAGTCCAAGGT
	CAAAAAGGGGGAAGAGAAATG

2. sgRNA sequences for CRIPSRi cell lines

Target	Sequence, 5' to 3'
ATF6 #1, #2	CCACCTTGTTGGTTAATATCTGGGACGGCGGGTTTAAGAGCTAAGCTG, CCACCTTGTTGGTATTAATCACGGAGTTCCAGTTTAAGAGCTAAGCTG
IRE1 #1, #2	CCACCTTGTTGGGGCGGTGACCGAGCCTCAGGTTTAAGAGCTAAGCTG, CCACCTTGTTGGAGCGGACGCAGAACTGACTGTTTAAGAGCTAAGCTG
PERK #1, #2	CCACCTTGTTGGACAGCCAGCCGTGTTCCCCGTTTAAGAGCTAAGCTG,

	CCACCTTGTTGGCGGGCTGAGACGTGGCCAGGTTTAAGAGCTAAGCTG
PKMYT1	CCACCTTGTTGGTCACGGGAGTCCTCCGCCCGTTTAAGAGCTAAGCTG, CCACCTTGTTGGGGCTGTTGCAGAAGAAGAGGTTTAAGAGCTAAGCTG

3. Primary antibodies

Antibody Target	**Company/Catalog #**	**Working dilution (WB)**	**Working dilution (FC/IF)**
BiP	Cell Signaling Technology, 3177S	1:1000	1:500
Calnexin	Cell Signaling Technology, 2679S	1:1000	1:500
PDIA3	Cell Signaling Technology, 3501P	1:1000	1:500

4. Secondary antibodies

Name	**Company/Catalog #**	**Working dilution (WB)**	**Working dilution (FC/IF)**
Mouse-HRP	BioRad, 1706516	1:2500	N/A
Rabbit-HRP	BioRad, 1706515	1:2500	N/A
AlexaFluor 588 anti-mouse	Invitrogen, A-11004	-	1:500
AlexaFluor 647 anti-rabbit	Invitrogen, A-21245	-	1:500

References

1. Acosta-Alvear, D. Unpublished results
2. Acosta-Alvear, D., Zhou, Y., Blais, A., Tsikitis, M., Lents, N.H., Arias, C., Lennon, C.J., Kluger, Y., and Dynlacht, B.D. (2007). XBP1 controls diverse cell type- and condition-specific transcriptional regulatory networks. Mol Cell 27, 53-66.
3. Adachi, Y., Kato, T., Yamada, T., Murata, D., Arai, K., Stahelin, R., Chan, D., Iijima, M. and Sesaki, H., 2020. Drp1 Tubulates the ER in a GTPase-Independent Manner. *Molecular Cell*, 80(4), pp.621-632.e6.
4. Alberts, B., 2008. *Molecular biology of the cell*. New York: Garland Science.
5. Appenzeller-Herzog, C. (2006). The ER-Golgi intermediate compartment (ERGIC): in search of its identity and function. Journal of Cell Science 119, 2173-2183.
6. Bae, D., Moore, K.A., Mella, J.M., Hayashi, S.Y., and Hollien, J. (2019). Degradation of Blos1 mRNA by IRE1 repositions lysosomes and protects cells from stress. J Cell Biol 218, 1118-1127.
7. Benmaamar, R., and Pagano, M. (2005). Involvement of the SCF Complex in the Control of Cdh1 Degradation in S-phase. Cell Cycle 4, 1230-1232.
8. Bergman, Z., Mclaurin, J., Eritano, A., Johnson, B., Sims, A. and Riggs, B., 2015. Spatial Reorganization of the Endoplasmic Reticulum during Mitosis Relies on Mitotic Kinase Cyclin A in the Early Drosophila Embryo. PLOS ONE, 10(2), p.e0117859.
9. V. Belyy, N.-H. Tran, P. Walter. Quantitative microscopy reveals dynamics and fate of clustered IRE1α. Proc. Natl. Acad. Sci. U.S.A. 117, 1533–1542 (2020).
10. Birky, C.W. (1983). The Partitioning of Cytoplasmic Organelles at Cell Division. In Aspects of Cell Regulation, J.F. Danielli, ed. (Academic Press), pp. 49-89.
11. Boettcher, B. and Barral, Y., 2013. The cell biology of open and closed mitosis. Nucleus, 4(3), pp.160-165.
12. Borel, F., Lacroix, F. and Margolis, R., 2002. Prolonged arrest of mammalian cells at the G_1/S boundary results in permanent S phase stasis. *Journal of Cell Science*, 115(14), pp.2829-2838.
13. Boulikas T., 1995. Phosphorylation of transcription factors and control of the cell cycle. Critical Review of Eukaryotic Gene Expression. 5(1)-77
14. Braakman, I., and Hebert, D.N. (2013). Protein Folding in the Endoplasmic Reticulum. Cold Spring Harbor Perspectives in Biology 5, a013201-a013201.
15. Cánepa, E.T., Scassa, M.E., Ceruti, J.M., Marazita, M.C., Carcagno, A.L., Sirkin, P.F., and Ogara, M.F. (2007). INK4 proteins, a family of mammalian CDK inhibitors with novel biological functions. IUBMB Life 59, 419-426.Ducommun et al 1991
16. Carreras-Sureda, A., Pihán, P., and Hetz, C. (2018). Calcium signaling at the endoplasmic reticulum: fine-tuning stress responses. Cell Calcium 70, 24-31.
17. Castro, A., Bernis, C., Vigneron, S., Labbé, J. and Lorca, T., 2005. The anaphase-promoting complex: a key factor in the regulation of cell cycle. *Oncogene*, 24(3), pp.314-325.
18. Cheffings, T., Burroughs, N. and Balasubramanian, M., 2016. Actomyosin Ring Formation and Tension Generation in Eukaryotic Cytokinesis. *Current Biology*, 26(15), pp.R719-R737.
19. Chen, C., Li, J., Qin, X. and Wang, W., 2020. Peroxisomal Membrane Contact Sites in Mammalian Cells. *Frontiers in Cell and Developmental Biology*, 8.

20. Colanzi, A., Carcedo, C.H., Persico, A., Cericola, C., Turacchio, G., Bonazzi, M., Luini, A., and Corda, D. (2007). The Golgi mitotic checkpoint is controlled by BARS dependent fission of the Golgi ribbon into separate stacks in G_2. 26, 2465-2476.
21. Collins, K., Jacks, T., and Pavletich, N.P. (1997). The cell cycle and cancer. Proceedings of the National Academy of Sciences 94, 2776.
22. Conlon, I., and Raff, M. (2003). Differences in the way a mammalian cell and yeast cells coordinate cell growth and cell-cycle progression. J Biol 2, 7-7.
23. Cross BC, Bond PJ, Sadowski PG, Jha BK, Zak J, Goodman JM, Silverman RH, Neubert TA, Baxendale IR, Ron D, Harding HP. The molecular basis for selective inhibition of unconventional mRNA splicing by an IRE1-binding small molecule. Proc Natl Acad Sci U S A. 2012 Apr 10;109(15):E869-78. doi: 10.1073/pnas.1115623109. Epub 2012 Feb 6. PMID: 22315414; PMCID: PMC3326519.
24. Costa-Mattioli M, Walter P. The integrated stress response: From mechanism to disease. Science. 2020 Apr 24;368(6489):eaat5314. doi: 10.1126/science.aat5314. PMID: 32327570.
25. Costello, J., Castro, I., Schrader, T., Islinger, M. and Schrader, M., 2017. Peroxisomal ACBD4 interacts with VAPB and promotes ER-peroxisome associations. *Cell Cycle*, 16(11), pp.1039-1045.
26. Coverley, D., Laman, H., and Laskey, R.A. (2002). Distinct roles for cyclins E and A during DNA replication complex assembly and activation. Nature Cell Biology 4,523-528.Jeffrey et al 1995
27. Cox, J.S., Shamu, C.E., and Walter, P. (1993). Transcriptional induction of genes encoding endoplasmic reticulum resident proteins requires a transmembrane protein kinase. Cell 73, 1197-1206.
28. Credle, J.J., Finer-Moore, J.S., Papa, F.R., Stroud, R.M., and Walter, P. (2005). On the mechanism of sensing unfolded protein in the endoplasmic reticulum.
29. Dufey, E., Bravo-San Pedro, J.M., Eggers, C., Gonzalez-Quiroz, M., Urra, H., Sagredo, A.I., Sepulveda, D., Pihan, P., Carreras-Sureda, A., Hazari, Y., et al. (2020). Genotoxic stress triggers the activation of IRE1alpha-dependent RNA decay to modulate the DNA damage response. Nat Commun 11, 2401.
30. Duran-Aniotz, C., Martínez, G., and Hetz, C. (2014). Memory loss in Alzheimer's disease: are the alterations in the UPR network involved in the cognitive impairment? 6.
31. Ellenberg, J., Siggia, E.D., Moreira, J.E., Smith, C.L., Presley, J.F., Worman, H.J., and Lippincott-Schwartz, J. (1997). Nuclear Membrane Dynamics and Reassembly in Living Cells: Targeting of an Inner Nuclear Membrane Protein in Interphase and Mitosis. The Journal of Cell Biology 138, 1193-1206.
32. Facchetti, G., Chang, F. and Howard, M., 2017. Controlling cell size through sizer mechanisms. *Current Opinion in Systems Biology*, 5, pp.86-92.
33. Fantes, P., and Nurse, P. (1977). Control of cell size at division in fission yeast by a growth-modulated size control over nuclear division. 107, 377-386.
34. Fesquet, D., Labbé, J.C., Derancourt, J., Capony, J.P., Galas, S., Girard, F., Lorca, T., Shuttleworth, J., Dorée, M., and Cavadore, J.C. (1993). The MO15 gene encodes the catalytic subunit of a protein kinase that activates cdc2 and other cyclin-dependent

kinases (CDKs) through phosphorylation of Thr161 and its homologues. The EMBO Journal 12, 3111-3121.Schmidt et al 2017 (wee1 family)
35. Friedman, J.R., Lackner, L.L., West, M., Dibenedetto, J.R., Nunnari, J., and Voeltz, G.K. (2011). ER Tubules Mark Sites of Mitochondrial Division. Science 334, 358-362.
36. Gallagher, C., Garri, C., Cain, E., Ang, K., Wilson, C., Chen, S., Hearn, B., Jaishankar, P., Aranda-Diaz, A., Arkin, M., Renslo, A. and Walter, P., 2016. Ceapins are a new class of unfolded protein response inhibitors, selectively targeting the ATF6α branch. eLife, 5.
37. Gao, G., Zhu, C., Liu, E. and Nabi, I., 2019. Reticulon and CLIMP-63 regulate nanodomain organization of peripheral ER tubules. *PLOS Biology*, 17(8), p.e3000355.
38. Gartel, A.L., and Tyner, A.L. (1999). Transcriptional Regulation of the p21(WAF1/CIP1)Gene. Experimental Cell Research 246, 280-289.Sherr and Roberts 1999
39. Gass, J. (2004). Stressed-out B cells? Plasma-cell differentiation and the unfolded protein response. 25, 17-24.
    Genomic Stability. DNA and Cell Biology.Macip et al 2006
40. Gerace, L., and Burke, B. (1988). Functional Organization of the Nuclear Envelope. Annual Review of Cell Biology 4, 335-374.
41. Gérard, C. and Goldbeter, A., 2014. The balance between cell cycle arrest and cell proliferation: control by the extracellular matrix and by contact inhibition. *Interface Focus*, 4(3), p.20130075.
42. Goméz-Puerta, S., Voigt, F., (2021) Live imaging of the co-translational recruitment of XBP1 mRNA to the ER and its processing by diffuse, non-polarized IRE1a. BioRxiv.
43. Gonzalez, T.N., Sidrauski, C., Dörfler, S., and Walter, P. (1999). Mechanism of nonspliceosomal mRNA splicing in the unfolded protein response pathway. 18, 3119 3132.
44. Gurel, P., Hatch, A. and Higgs, H., 2014. Connecting the Cytoskeleton to the Endoplasmic Reticulum and Golgi. *Current Biology*, 24(14), pp.R660-R672.
45. Halbleib, K., Pesek, K., Covino, R., Hofbauer, H., Wunnicke, D., Hänelt, I., Hummer, G. and Ernst, R., 2017. Activation of the Unfolded Protein Response by Lipid Bilayer Stress. *Molecular Cell*, 67(4), pp.673-684.e8.
46. Harding, H., Zhang, Y. and Ron, D., 1999. Protein translation and folding are coupled by an endoplasmic-reticulum-resident kinase. *Nature*, 397(6716), pp.271-274.
47. Harnoss, J.M., Le Thomas, A., Shemorry, A., Marsters, S.A., Lawrence, D.A., Lu, M., Chen, Y.-C.A., Qing, J., Totpal, K., Kan, D., et al. (2019). Disruption of IRE1α through its kinase domain attenuates multiple myeloma. Proceedings of the National Academy of Sciences 116, 16420-16429.
48. Hashida, K., Kitao, Y., Sudo, H., Awa, Y., Maeda, S., Mori, K., Takahashi, R., Iinuma, M., and Hori, O. (2012). ATF6alpha Promotes Astroglial Activation and Neuronal Survival in a Chronic Mouse Model of Parkinson's Disease. 7, e47950.
49. Haze, K., Yoshida, H., Yanagi, H., Yura, T., and Mori, K. (1999). Mammalian Transcription Factor ATF6 Is Synthesized as a Transmembrane Protein and Activated by Proteolysis in Response to Endoplasmic Reticulum Stress. 10, 3787-3799.
50. Hetz, C., and Mollereau, B. (2014). Disturbance of endoplasmic reticulum proteostasis in neurodegenerative diseases. Nature Reviews Neuroscience 15, 233-249.

51. Hetz, C., Zhang, K., & Kaufman, R. J. (2020). Mechanisms, regulation and functions of the unfolded protein response. *Nature Reviews Molecular Cell Biology*, *21*(8), 421–438.
52. Hetzer, M.W., Walther, T.C., and Mattaj, I.W. (2005). PUSHING THE ENVELOPE: Structure, Function, and Dynamics of the Nuclear Periphery. 21, 347-380.
53. Ho, N., Yap, W.S., Xu, J., Wu, H., Koh, J.H., Goh, W.W.B., George, B., Chong, S.C., Taubert, S., and Thibault, G. (2020). Stress sensor Ire1 deploys a divergent transcriptional program in response to lipid bilayer stress. J Cell Biol 219.
54. Hollien, J., Lin, J.H., Li, H., Stevens, N., Walter, P., and Weissman, J.S. (2009). Regulated Ire1-dependent decay of messenger RNAs in mammalian cells. Journal of Cell Biology 186, 323-331.
55. Hu, H., Tian, M., Ding, C. and Yu, S., 2019. The C/EBP Homologous Protein (CHOP) Transcription Factor Functions in Endoplasmic Reticulum Stress-Induced Apoptosis and Microbial Infection. *Frontiers in Immunology*, 9.
56. Hunter, T., and Pines, J. (1994). Cyclins and cancer II: Cyclin D and CDK inhibitors come of age. Cell 79, 573-582.Besson et al 2008 (cdk inhibitors stressors)
57. Ishikawa K., I.H., Saito T. (2007). Damage-Dependent Cell Cycle Checkpoints and
58. Jelsema, C.L., and Morré, D.J. (1978). Distribution of phospholipid biosynthetic enzymes among cell components of rat liver. Journal of Biological Chemistry 253, 7960-7971.
59. Jokitalo, E., Cabrera-Poch, N., Warren, G. and Shima, D., 2001. Golgi clusters and vesicles mediate mitotic inheritance independently of the endoplasmic reticulum. *Journal of Cell Biology*, 154(2), pp.317-330.
60. Karagöz, G.E., Acosta-Alvear, D., Nguyen, H.T., Lee, C.P., Chu, F., and Walter, P. (2017). *An unfolded protein-induced conformational switch activates mammalian IRE1. eLife 6.*
61. Karagöz GE, Aragón T and Acosta-Alvear D. Recent advances in signal integration mechanisms in the unfolded protein response [version 1; peer review: 2 approved] F1000Research 2019, 8(F1000 Faculty Rev):1840 (https://doi.org/10.12688/f1000research.19848.1)
62. Kato, J., Matsushime, H., Hiebert, S.W., Ewen, M.E., and Sherr, C.J. (1993). Direct
63. Killander, D., and Zetterberg, A. (1965a). A quantitative cytochemical investigation of the relationship between cell mass and initiation of DNA synthesis in mouse fibroblasts in vitro. 40, 12-20.
64. Kirk, S.J., Cliff, J.M., Thomas, J.A., and Ward, T.H. (2010). Biogenesis of secretory organelles during B cell differentiation. 87, 245-255.
65. Koh, S.-B., Mascalchi, P., Rodriguez, E., Lin, Y., Jodrell, D.I., Richards, F.M., and Lyons, S.K. (2017). A quantitative FastFUCCI assay defines cell cycle dynamics at a single-cell level. Journal of Cell Science 130, 512-520.
66. Korennykh, A.V., Korostelev, A.A., Egea, P.F., Finer-Moore, J., Stroud, R.M., Zhang, C., Shokat, K.M., and Walter, P. (2011). Structural and functional basis for RNA cleavage by Ire1. BMC Biology 9, 47.
67. Kornmann, B., Currie, E., Collins, S.R., Schuldiner, M., Nunnari, J., Weissman, J.S., and Walter, P. (2009). An ER-Mitochondria Tethering Complex Revealed by a Synthetic Biology Screen. Science 325, 477-481.

68. Kosmaczewski, S.G., Edwards, T.J., Han, S.M., Eckwahl, M.J., Meyer, B.I., Peach, S., Hesselberth, J.R., Wolin, S.L., and Hammarlund, M. (2014). The R tc B RNA ligase is an essential component of the metazoan unfolded protein response. EMBO reports 15, 1278-1285.
69. Kozlov, G. and Gehring, K., 2020. Calnexin cycle – structural features of the ER chaperone system. *The FEBS Journal*, 287(20), pp.4322-4340.
70. Lee, J.E., Cathey, P.I., Wu, H., Parker, R., and Voeltz, G.K. (2020). Endoplasmic reticulum contact sites regulate the dynamics of membraneless organelles. Science 367, eaay7108.
71. Lewis SC, Uchiyama LF, Nunnari J. ER-mitochondria contacts couple mtDNA synthesis with mitochondrial division in human cells. Science. 2016 Jul 15;353(6296):aaf5549. doi: 10.1126/science.aaf5549. PMID: 27418514; PMCID: PMC5554545.
72. Lim, C., Davis, O., Shin, H., Zhang, J., Berdan, C., Jiang, X., Counihan, J., Ory, D., Nomura, D. and Zoncu, R., 2019. ER–lysosome contacts enable cholesterol sensing by mTORC1 and drive aberrant growth signalling in Niemann–Pick type C. *Nature Cell Biology*, 21(10), pp.1206-1218.
73. Liu, F., Stanton, J.J., Wu, Z., and Piwnica-Worms, H. (1997). The human Myt1 kinase preferentially phosphorylates Cdc2 on threonine 14 and localizes to the endoplasmic reticulum and Golgi complex. Molecular and cellular biology 17, 571-583.
74. Loud, A.V. (1968). A quantitative stereological description of the ultrastructure of normal rat liver parenchymal cells. The Journal of cell biology 37, 27-46.
75. Lowe, M., Gonatas, N. and Warren, G., 2000. The Mitotic Phosphorylation Cycle of the Cis-Golgi Matrix Protein Gm130. *Journal of Cell Biology*, 149(2), pp.341-356.
76. Lu, M., Lawrence, D.A., Marsters, S., Acosta-Alvear, D., Kimmig, P., Mendez, A.S., Paton, A.W., Paton, J.C., Walter, P., and Ashkenazi, A. (2014a). Opposing unfolded-protein-response signals converge on death receptor 5 to control apoptosis. Science 345, 98-101.
77. Lu, Y., Liang, F.-X., and Wang, X. (2014b). A Synthetic Biology Approach Identifies the Mammalian UPR RNA Ligase RtcB. 55, 758-770.
78. Maller, J.L., Gautier, J., Langan, T.A., Lohka, M.J., Shenoy, S., Shalloway, D., and Nurse, P. (1989). Maturation-promoting factor and the regulation of the cell cycle. 1989, 53-63.
79. Manford, A.G., Stefan, C.J., Yuan, H.L., MacGurn, J.A., and Emr, S.D. (2012). ER to Plasma Membrane Tethering Proteins Regulate Cell Signaling and ER Morphology. Developmental Cell 23, 1129-1140.
80. Marciniak, S.J., Garcia-Bonilla, L., Hu, J., Harding, H.P., and Ron, D. (2006). Activation-dependent substrate recruitment by the eukaryotic translation initiation factor 2 kinase PERK. 172, 201-209.
81. Matus, S., Valenzuela, V., Medinas, D.B., and Hetz, C. (2013). ER Dysfunction and Protein Folding Stress in ALS. 2013, 1-12.
82. Moore, A., Coscia, S., Simpson, C., Ortega, F., Wait, E., Heddleston, J., Nirschl, J., Obara, C., Guedes-Dias, P., Boecker, C., Chew, T., Theriot, J., Lippincott-Schwartz, J. and Holzbaur, E., 2021. Actin cables and comet tails organize mitochondrial networks in mitosis. *Nature*, 591(7851), pp.659-664.

83. Nadanaka, S., Okada, T., Yoshida, H., and Mori, K. (2007). Role of Disulfide Bridges Formed in the Luminal Domain of ATF6 in Sensing Endoplasmic Reticulum Stress. Molecular and Cellular Biology 27, 1027-1043.
84. Nakajima, H., Yonemura, S., Murata, M., Nakamura, N., Piwnica-Worms, H., and Nishida, E. (2008a). Myt1 protein kinase is essential for Golgi and ER assembly during mitotic exit. Journal of Cell Biology 181, 89-103.
85. Newport, J.W., and Forbes, D.J. (1987). The Nucleus: Structure, Function, and Dynamics. 56, 535-565.
86. Ni, M., and Lee, A.S. (2007). ER chaperones in mammalian development and human diseases. FEBS Lett 581, 3641-3651.
87. Nishitani, H., Lygerou, Z., Nishimoto, T., and Nurse, P. (2000). The Cdt1 protein is required to license DNA for replication in fission yeast. Nature 404, 625-628.
88. Olzmann, J.A., and Carvalho, P. (2019). Dynamics and functions of lipid droplets. Nature Reviews Molecular Cell Biology 20, 137-155.
89. Ouellet, J. and Barral, Y., 2012. Organelle segregation during mitosis: Lessons from asymmetrically dividing cells. *Journal of Cell Biology*, 196(3), pp.305-313.
90. Parakh, S. and Atkin, J., 2015. Novel roles for protein disulphide isomerase in disease states: a double edged sword?. *Frontiers in Cell and Developmental Biology*
91. Pardee, A., 1974. A Restriction Point for Control of Normal Animal Cell Proliferation. *Proceedings of the National Academy of Sciences*, 71(4), pp.1286-1290.
92. Peschek, J., Acosta-Alvear, D., Mendez, A.S., and Walter, P. (2015). A conformational RNA zipper promotes intron ejection during non-conventional XBP1 mRNA splicing. EMBO reports 16, 1688-1698.
93. Pincus, D., Chevalier, M.W., Aragon, T., van Anken, E., Vidal, S.E., El-Samad, H., and Walter, P. (2010). BiP binding to the ER-stress sensor Ire1 tunes the homeostatic behavior of the unfolded protein response. PLoS Biol 8, e1000415.
94. Pinton, P., Giorgi, C., Siviero, R., Zecchini, E. and Rizzuto, R., 2008. Calcium and apoptosis: ER-mitochondria Ca2+ transfer in the control of apoptosis. *Oncogene*, 27(50), pp.6407-6418.
95. Prostko, C.R., Brostrom, M.A., and Brostrom, C.O. (1993). Reversible phosphorylation of eukaryotic initiation factor 2? in response to endoplasmic reticular signaling. 127-128, 255-265.
96. Qi, L., Larson, M., Gilbert, L., Doudna, J., Weissman, J., Arkin, A. and Lim, W., 2021. Repurposing CRISPR as an RNA-guided platform for sequence-specific control of gene expression. *Cell*, 184(3), p.844.
97. Qi, L., Tsai, B., and Arvan, P. (2017). New Insights into the Physiological Role of Endoplasmic Reticulum-Associated Degradation. Trends in Cell Biology 27, 430-440.
98. Rishal, I. and Fainzilber, M., 2019. Cell size sensing—a one-dimensional solution for a three-dimensional problem?. *BMC Biology*, 17(1).
99. Rohde, J., Heitman, J., and Cardenas, M.E. (2001). The TOR Kinases Link Nutrient Sensing to Cell Growth. 276, 9583-9586.
100. Roussel, B.D., Kruppa, A.J., Miranda, E., Crowther, D.C., Lomas, D.A., and Marciniak, S.J. (2013). Endoplasmic reticulum dysfunction in neurological disease. 12, 105-118.

101. Rowland, A.A., Chitwood, P.J., Phillips, M.J., and Voeltz, G.K. (2014). ER Contact Sites Define the Position and Timing of Endosome Fission. Cell 159, 1027-1041.
102. Rozpedek, W., Pytel, D., Mucha, B., Leszczynska, H., Diehl, J. and Majsterek, I., 2016. The Role of the PERK/eIF2α/ATF4/CHOP Signaling Pathway in Tumor Progression During Endoplasmic Reticulum Stress. *Current Molecular Medicine*, 16(6), pp.533-544.
103. Russell, P., and Nurse, P. (1987). Negative regulation of mitosis by wee1+, a gene encoding a protein kinase homolog. 49, 559-567.
104. Sakaue-Sawano, A., Kurokawa, H., Morimura, T., Hanyu, A., Hama, H., Osawa, H., Kashiwagi, S., Fukami, K., Miyata, T., Miyoshi, H., et al. (2008). Visualizing Spatiotemporal Dynamics of Multicellular Cell-Cycle Progression. Cell 132, 487-498.
105. Satyanarayana, A. and Kaldis, P., 2009. Mammalian cell-cycle regulation: several Cdks, numerous cyclins and diverse compensatory mechanisms. *Oncogene*, 28(33), pp.2925-2939.
106. Scheuner, D., Song, B., McEwen, E., Liu, C., Laybutt, R., Gillespie, P., Saunders, T., Bonner-Weir, S., and Kaufman, R.J. (2001). Translational Control Is Required for the Unfolded Protein Response and In Vivo Glucose Homeostasis. Molecular Cell 7, 1165-1176.
107. Scorrano, L., De Matteis, M., Emr, S., Giordano, F., Hajnóczky, G., Kornmann, B., Lackner, L., Levine, T., Pellegrini, L., Reinisch, K., Rizzuto, R., Simmen, T., Stenmark, H., Ungermann, C. and Schuldiner, M., 2019. Coming together to define membrane contact sites. *Nature Communications*, 10(1).
108. Seyb, K., Ansar, S., Bean, J. and Michaelis, M., 2006. β-Amyloid and Endoplasmic Reticulum Stress Reponses in Primary Neurons: Effects of Drugs That Interact With the Cytoskeleton. *Journal of Molecular Neuroscience*, 28(2), pp.111-124.
109. Shahriyari, L. and Komarova, N., 2013. Symmetric vs. Asymmetric Stem Cell Divisions: An Adaptation against Cancer?. *PLoS ONE*, 8(10), p.e76195.
110. Shen, K., Arslan, S., Akopian, D., Ha, T. and Shan, S., 2013. Activated GTPase movement on an RNA scaffold drives cotranslational protein targeting. *The FASEB Journal*, 27(S1).
111. Shibata, Y., Shemesh, T., Prinz, W.A., Palazzo, A.F., Kozlov, M.M., and Rapoport, T.A. (2010). Mechanisms Determining the Morphology of the Peripheral ER. 143, 774-788.
112. Shibata, Y., Voeltz, G.K., and Rapoport, T.A. (2006). Rough Sheets and Smooth Tubules. Cell 126, 435-439.
113. Shima, D.T., Cabrera-Poch, N., Pepperkok, R., and Warren, G. (1998). An Ordered Inheritance Strategy for the Golgi Apparatus: Visualization of Mitotic Disassembly Reveals a Role for the Mitotic Spindle. Journal of Cell Biology 141, 955-966.
114. Solley, S. C. Roles of the Unfolded Protein Response in the Mammalian Cell Cycle. MA Thesis. UCSB 2020
115. Soullam, B., and Worman, H.J. (1995). Signals and structural features involved in integral membrane protein targeting to the inner nuclear membrane. The Journal of Cell Biology 130, 15-27.

116. Sriburi, R., Jackowski, S., Mori, K., and Brewer, J.W. (2004). XBP1: a link between the unfolded protein response, lipid biosynthesis, and biogenesis of the endoplasmic reticulum. J Cell Biol 167, 35-41.
117. Suzuki K, Takahashi K. Reduced cell adhesion during mitosis by threonine phosphorylation of beta1 integrin. J Cell Physiol. 2003 Nov;197(2):297-305. doi: 10.1002/jcp.10354. PMID: 14502569.
118. Uchiyama, Y. and Asari, A., 1984. A morphometric study of the variations in subcellular structures of rat hepatocytes during 24 hours. *Cell and Tissue Research*, 236(2).
119. Uhlén, M., Fagerberg, L., Hallström, B.M., Lindskog, C., Oksvold, P., Mardinoglu, A., Sivertsson, Å., Kampf, C., Sjöstedt, E., Asplund, A., et al. (2015). Tissue-based map of the human proteome. Science 347, 1260419.
120. Vattem, K.M., and Wek, R.C. (2004). Reinitiation involving upstream ORFs regulates ATF4 mRNA translation in mammalian cells. Proceedings of the National Academy of Sciences 101, 11269-11274.
121. Vidal, R.L., and Hetz, C. (2012). Crosstalk between the UPR and autophagy pathway contributes to handling cellular stress in neurodegenerative disease. 8, 970-972.
122. Vodermaier, H.C. (2004). APC/C and SCF: Controlling Each Other and the Cell Cycle. Curr Biol 14, R787-R796.
123. Robert G. Abrisch, Samantha C. Gumbin, Brett Taylor Wisniewski, Laura L. Lackner, Gia K. Voeltz; Fission and fusion machineries converge at ER contact sites to regulate mitochondrial morphology. *J Cell Biol* 6 April 2020; 219 (4): e201911122. doi: https://doi.org/10.1083/jcb.201911122
124. Walter, P., and Blobel, G. (1981). Translocation of proteins across the endoplasmic reticulum III. Signal recognition protein (SRP) causes signal sequence-dependent and site-specific arrest of chain elongation that is released by microsomal membranes. The Journal of Cell Biology 91, 557-561.
125. Walter, P., and Ron, D. (2011). The Unfolded Protein Response: From Stress Pathway to Homeostatic Regulation. Science 334, 1081-1086.
126. Wang, S. and Kaufman, R., 2012. The impact of the unfolded protein response on human disease. *Journal of Cell Biology*, 197(7), pp.857-867.
127. Warren, G., and Wickner, W. (1996). Organelle Inheritance. 84, 395-400.
128. Wei, W., Ayad, N.G., Wan, Y., Zhang, G.-J., Kirschner, M.W., and Kaelin, W.G. (2004). Degradation of the SCF component Skp2 in cell-cycle phase G_1 by the anaphase-promoting complex. Nature 428, 194-198.
129. Weinberg et. al. 1995. Binding of cyclin D to the retinoblastoma gene product (pRb) E2F Cyclin E and A, S phase
130. Werstuck, G., Lentz, S., Dayal, S., Hossain, G., Sood, S., Shi, Y., Zhou, J., Maeda, N., Krisans, S., Malinow, M. and Austin, R., 2001. Homocysteine-induced endoplasmic reticulum stress causes dysregulation of the cholesterol and triglyceride biosynthetic pathways. *Journal of Clinical Investigation*, 107(10), pp.1263-1273.
131. Xeros, N., 1962. Deoxyriboside Control and Synchronization of Mitosis. *Nature*, 194(4829), pp.682-683.
132. Yamamoto, K., Sato, T., Matsui, T., Sato, M., Okada, T., Yoshida, H., Harada, A. and Mori, K., 2007. Transcriptional Induction of Mammalian ER Quality Control

Proteins Is Mediated by Single or Combined Action of ATF6α and XBP1. *Developmental Cell*, 13(3), pp.365-376.

133. Yamamoto, K., Sato, T., Matsui, T., Sato, M., Okada, T., Yoshida, H., Harada, A., and Mori, K. (2007). Transcriptional Induction of Mammalian ER Quality Control Proteins Is Mediated by Single or Combined Action of ATF6α and XBP1. 13, 365-376.
134. Yarapureddy, S., Abril, J., Foote, J., Kumar, S., Asad, O., Sharath, V., Faraj, J., Daniel, D., Dickman, P., White-Collins, A., Hingorani, P. and Sertil, A., 2019. ATF6α Activation Enhances Survival against Chemotherapy and Serves as a Prognostic Indicator in Osteosarcoma. *Neoplasia*, 21(6), pp.516-532.
135. Ye, J., Rawson, R.B., Komuro, R., Chen, X., Davé, U.P., Prywes, R., Brown, M.S., and Goldstein, J.L. (2000). ER Stress Induces Cleavage of Membrane-Bound ATF6 by the Same Proteases that Process SREBPs. Molecular Cell 6, 1355-1364.
136. Yeong, F., 2013. Multi-step down-regulation of the secretory pathway in mitosis: A fresh perspective on protein trafficking. *BioEssays*, 35(5), pp.462-471.
137. Yoshida, H. (1998). Identification of the cis-Acting Endoplasmic Reticulum Stress Response Element Responsible for Transcriptional Induction of Mammalian Glucose-regulated Proteins. INVOLVEMENT OF BASIC LEUCINE ZIPPER TRANSCRIPTION FACTORS. 273, 33741-33749.
138. Zappa, F. (2021) Signaling by the integrated stress response kinase PKR is fine-tuned by dynamic clustering. BioRxiv.